

SEMI-ANNUAL
TECHNICAL REPORT

to the

AIR FORCE OFFICE OF SCIENTIFIC RESEARCH

from

Eugene Herrin

Geophysical Laboratory
Institute for the Study
of Earth and Man
Southern Methodist University

For the period ending March 1, 1976

ADA 112668

ARPA Order: 2382
Program Code: 4F10
Name of Contractor: Southern Methodist University
Effective Date of Contract: January 16, 1974
Contract Expiration Date: July 15, 1976
Amount of Contract Dollars: \$711,731
Contract Number: F 44620-73-C-0044,
Principal Investigator and Phone Number: Eugene Herrin,
#214-692-2760
Program Manager and Phone Number: Truman Cook, Director of
Research Administration,
#214-692-2031
Title of Work: Improved Methods for Detection of Long Period
Rayleigh Waves and for Identification of
Earthquakes and Underground Explosions

DTIC FILE COPY

Sponsored by
Advanced Research Projects Agency
ARPA Order No. 2382

DTIC
ELECTE
S MAR 30 1982 D
D

APPROVED FOR PUBLIC RELEASE
DISTRIBUTION UNLIMITED

82 03 30 070

LINEAR HIGH RESOLUTION FREQUENCY-WAVENUMBER ANALYSIS

by

EUGENE SMART

Accession For	
NTIS GRA&I	<input checked="" type="checkbox"/>
DTIC TAB	<input type="checkbox"/>
Unannounced	<input type="checkbox"/>
Justification	
By	
Distribution/	
Availability Codes	
Dist	Avail and/or Special
A	



Geophysical Laboratory
Institute for the Study
of Earth and Man
Southern Methodist University
Dallas, Texas 75275

ABSTRACT

The marginal success of the several high-resolution frequency-wavenumber ($f - k$) techniques to date is cited from the literature. Their ability to resolve signals from two closely spaced sources is not markedly superior to that of ordinary beamforming. Moreover, such non-linear techniques yield distorted magnitudes and azimuths. The ordinary $f - k$ "spectrum" is shown to be no more than a 1-signal estimator, and the existing high resolution techniques to be but variations of that 1-signal estimator. In this paper the notion of the wavenumber "spectrum" is set aside. Instead, by analogy to the 1-signal estimator (the ordinary $f - k$ "spectrum"), a linear M -signal estimator is developed. The high resolving power of this technique and the fidelity of its estimates is demonstrated theoretically and by computer examples both real and synthetic.

Introduction

The mathematical development of linear high-resolution frequency-wave number analysis was presented in the Semi-annual report to AFOSR for the period ending 1 March 1975. Since that time the software implementation of the theory has been accomplished and the technique has been applied to explosion and earthquake signals recorded at the Large Aperture Seismic Array (LASA) in Montana. The application of the technique to real data is the basis for this report, although for the purposes of completeness and continuity the previously-reported section on mathematical development is also included.

The frequency-wavenumber spectrum, which is a multi-dimensional equivalent of the ordinary frequency spectrum, is used in the sciences for theoretical and experimental analysis of traveling waves. It was introduced formally into seismology by Burg (5) in an application to data analysis. The ordinary unsmoothed three dimensional frequency-wavenumber spectrum of time series data sampled at discrete points in space is given by

$$P(\omega, \bar{k}) = \left| \frac{1}{N} \sum_{n=1}^N \left\{ A_n(\omega) \exp[i\alpha_n(\omega)] \right\} \cdot \exp(i\bar{k} \cdot \bar{r}_n) \right|^2 \quad (1)$$

where

n is the index of the spatial sample points.

$A_n(\omega) \exp[i\alpha_n(\omega)]$

is the finite Fourier transform of the n th time series.

\bar{k}

is the vector wavenumber.

\bar{r}_n

is the vector location of the n th sensor, or sample point.

Each Fourier transform term is equivalent to a sinusoid.

For example, the sinusoid for the n th transform at frequency

ω has amplitude $A_n(\omega)$ and phase $\alpha_n(\omega)$

(at the center of the time window).

Now $-\bar{k} \cdot \bar{r}_n$ is the phase delay, between the origin

and \bar{r}_n , of a plane wave arriving from the azimuth of the vector \bar{k} and traveling at the phase velocity

$$v = \omega/|\bar{k}|$$

So, multiplication of the transform by the kernel $\exp(i\bar{k}\cdot\bar{r}_n)$ has the effect of advancing the sinusoid by just the amount the wave itself had delayed it. Thus the summation in (1), above, is a beam sum, and the f - k spectrum is just the frequency domain equivalent of ordinary beam steering.

When the traveling-wave delays are exactly compensated for by the beam shifting, i.e., when the true \bar{k} of the signal is selected, the sinusoids add up constructively with no interference, and the power, P , is maximized. Within certain limits, then, maxima or peaks in f - k space are treated as indications of the presence of traveling plane waves, and the location and size of the maxima are taken as estimates of the speed, bearing, frequency, and power of those signals. If more than one signal is present or if there is noise in the data, though exact determinations are no longer possible, the f - k spectrum is still useful for detecting and estimating signals, again within limits.

One of those limitations is imposed by the finite width of the maxima associated with signals. (9) The case is analogous to that of the ordinary frequency spectrum in which components are represented by peaks of finite width.

Plane wave signal peaks in the $f-k$ spectrum have a half-power width of the order

$$\Delta k \approx \frac{1}{\Delta X}$$

where ΔX is the width, or aperture, of the array of spatial sample points. (4) If two signals in the same time window and frequency band are also close enough in phase velocity and azimuth so their wavenumbers, say \bar{k}_1 and \bar{k}_2 , are such:

$$|\bar{k}_1 - \bar{k}_2| < \Delta k,$$

then their maxima in the $f-k$ spectrum are merged and form a single peak. (23) Thus, because the sensor arrays are spatially finite their resolving power is finite. Attempts to increase that power of resolution through data processing technique have required mathematical schemes to reduce the width of the lobe of the signal peak (1-3, 6-15, 17, 19). However, the straight-forward geometric appeal of this approach has proved misleading thus far. In such hybrid spectra signal lobe-widths indeed have been narrowed substantially. Nevertheless, when signal pairs approach each other in the k -plane, resolution still fails as the separation nears Δk , to wit, the lobe half-width for the ordinary $f-k$ spectrum. (2, 11, 13, 15, 20).

Observations of other investigators on the shortcomings of various high-resolution frequency-wavenumber techniques are cited below.

Lintz (15) finds that the high-resolution f-k spectral technique of Haney (14) does not significantly improve the capability of a seismic array to detect multiple time-overlapping events from different azimuths.

Galat and Sax (13) experimentally find the high-resolution f-k spectrum of Haney (14), and that of Capon (8), (9), no better at resolving two simultaneously arriving waves than the ordinary f-k spectrum. McCowan and Lintz (17) call attention to an unrecoverable distortion of the true amplitude spectrum in Haney's technique, and the marked disadvantage of spurious peaks under certain conditions which they regard as the inevitable result of using a high-gain procedure.

Seligson (20) describes conditions under which Capon's high-resolution technique displays less "angular resolution" than ordinary beamforming. McDonough (18) concludes that variations in amplitude from sensor to sensor may be expected to produce anomalous behavior in Capon's processor. Of course, just such variation in amplitude from sensor to sensor will result precisely because of the presence of two or more signals. McDonough offers arguments to show that ordinary beamforming is less susceptible to instability resulting from

small signal modeling errors than all other array processors.

Haney, too, notes that in the processor he describes (14) variation in amplitude from sensor-to-sensor could distort the spectrum beyond recognition. He remedies this difficulty by forcing the same amplitude upon each input channel, thus destroying the very amplitude information that would be indicative of the presence of two or more signals.

Woods and Lintz (23) conclude that given favorable conditions, the resolving power of the maximum-likelihood f-k spectrum can be effectively infinite, but, disappointingly, offer computer examples on synthetic data in which the input signal pairs are well spaced to begin with (they are separated by a distance of 0.9 of the main-lobe half-width). Cox (11) also offers theory suggesting that given arbitrarily high signal-to-noise ratios arbitrarily fine resolution should be possible, but he does not offer a method.

It may be argued that the limited resolving power of the several high-resolution techniques results from the wavenumber spectrum being in reality a 1-signal estimator. Indeed the ordinary f-k "spectrum" is a least squares estimator for fitting data to a single plane wave, as shown further on. In routine automated processing of the LASA LP data Mack and Smart (24) found the ordinary spectrum useful for estimating only one signal at a time. Estimates of a possible second

signal were made by recomputing the wavenumber spectrum after the first (and larger) estimate had been subtracted from the data. They call this process stripping; it is useful, of course, only for estimating signals separated by about the reciprocal of the array diameter or more. At that, such estimates of a pair of signals are not optimum, but first order approximations.

Properly, the f - k spectrum is defined only for signals of infinite spatial extent traversing infinitely large arrays. The effect of a signal of wavenumber k is then confined to the point k in the spectrum. Approximations to this definition are useful if the dimensions of signals and arrays are sufficiently large. Failing that, the "spectrum" reduces to a 1-signal estimator as noted. While the high-resolution techniques do attempt to extend the effective array diameter, they all test the wavenumber space with a 1-signal probe, as in the ordinary f - k spectrum.

It is proposed here to set aside the notion of a spectrum. Rather we will extend the 1-signal estimator to an M -signal estimator thus to permit the simultaneous removal of the effects of one signal from the estimate of another and so achieve true high-resolution. At the same time, use of simple beamforming (in the k -plane) to estimate each of the M signals will preserve the stability and estimate fidel-

ity of the ordinary f-k spectrum.

In the following discussion a 1-signal least squares estimator is developed and is identified with the ordinary f-k spectrum. Analogy to the 1-signal estimator is used to develop an M-signal estimator.

Conventional Frequency-Wavenumber Analysis

In the conventional frequency-wavenumber spectrum (ordinary or high-resolution) a single plane wave is hypothesized at each frequency. That model is then tested over the wavenumber space of interest. One attempts to minimize the error

$$\epsilon = \sum_{n=1}^N \left| U_n - A e^{i\vec{k} \cdot \vec{r}_n} \right|^2$$

by varying A and \vec{k} where

U_n	are the complex Fourier series terms (for the given frequency)
n	is the sensor, or channel, index
N	is the total number of sensors
\vec{r}_n	are the location vectors of the sensors
A	is the complex Fourier series term for the hypothesized plane wave (at the given frequency)
\vec{k}	is the wavenumber of the hypothetical plane wave (at that given frequency)

$A e^{i\vec{k}\cdot\vec{r}_n}$, $n = 1, \dots, N$ is the model, i.e., the hypothesized plane wave.

Note that also one can write ϵ as

$$\epsilon = \sum_{n=1}^N \left| U_n e^{-i\vec{k}\cdot\vec{r}_n} - A \right|^2$$

since $|e^{-i\vec{k}\cdot\vec{r}_n}| = 1$.

For a given \vec{k} , ϵ is minimized by setting A to

$$A = \frac{1}{N} \sum_{n=1}^N U_n e^{-i\vec{k}\cdot\vec{r}_n}$$

which is shown by the following:

$$\begin{aligned} \text{Let} \quad a_n + i c_n &\equiv U_n e^{-i\vec{k}\cdot\vec{r}_n} \\ \text{and} \quad a + i c &\equiv A \end{aligned}$$

Then

$$\begin{aligned} \epsilon &= \sum_{n=1}^N \left| (a_n - a) + i(c_n - c) \right|^2 \\ &= \sum_{n=1}^N (a_n - a)^2 + (c_n - c)^2 \end{aligned}$$

Take partial derivatives:

$$\frac{\partial \epsilon}{\partial a} = -2 \sum_{n=1}^N (a_n - a); \quad \frac{\partial \epsilon}{\partial c} = -2 \sum_{n=1}^N (c_n - c)$$

$$\frac{\partial^2 \epsilon}{\partial a^2} = \frac{\partial^2 \epsilon}{\partial c^2} = 2N$$

Setting $\frac{\partial \epsilon}{\partial a} = \frac{\partial \epsilon}{\partial c} = 0$,

$$a = \frac{1}{N} \sum_{n=1}^N a_n \quad c = \frac{1}{N} \sum_{n=1}^N c_n$$

and

$$a + ic = A = \frac{1}{N} \sum_{n=1}^N (a_n + ic_n) = \frac{1}{N} \sum_{n=1}^N U_n e^{-i\vec{k} \cdot \vec{r}_n}$$

So, minimized with respect to A ,

$$\epsilon = \sum_{n=1}^N \left| U_n e^{-i\vec{k} \cdot \vec{r}_n} - \frac{1}{N} \sum_{j=1}^N U_j e^{-i\vec{k} \cdot \vec{r}_j} \right|^2$$

This expression can be separated into 2 parts, thus:

$$\begin{aligned} \epsilon &= \sum_{n=1}^N (a_n - a)^2 + (c_n - c)^2 \\ &= \sum_{n=1}^N a_n^2 - 2a_n a + a^2 + c_n^2 - 2c_n c + c^2 \\ &= \sum_{n=1}^N (a_n^2 + c_n^2) - 2a \cdot aN + a^2 N - 2c \cdot cN + c^2 N \\ &= \sum_{n=1}^N |a_n + ic_n|^2 - \frac{1}{N} \left| \sum_{n=1}^N a_n + ic_n \right|^2 \end{aligned}$$

Thus,

$$\epsilon = \sum_{n=1}^N |U_n|^2 - \frac{1}{N} \left| \sum_{n=1}^N U_n e^{-i\vec{k} \cdot \vec{r}_n} \right|^2$$

The second term is the ordinary frequency-wavenumber spectrum

$$P(f, \vec{k}) = \frac{1}{N} \left| \sum_{n=1}^N U_n(f) e^{-i\vec{k} \cdot \vec{r}_n} \right|^2$$

So,

$$\epsilon = \sum_{n=1}^N |U_n|^2 - P(\vec{k})$$

Since ϵ is a squared modulus

$$\epsilon \geq 0$$

and

$$\sum_{n=1}^N |U_n|^2 \geq 0$$

since it is a sum of squared moduli.

Similarly

$$P(\vec{k}) \geq 0$$

Since

$$\sum_{n=1}^N |U_n|^2 - P(\vec{k}) \geq 0,$$

$$\sum_{n=1}^N |U_n|^2 \geq P(\vec{k})$$

So to minimize ϵ one must maximize $P(\vec{k})$.

$$\epsilon(\vec{k}) = \sum_{n=1}^N \left| U_n e^{-i\vec{k} \cdot \vec{r}_n} - A \right|^2$$

becomes exactly zero when

$$U_n = e^{i\vec{k} \cdot \vec{r}_n} \cdot \frac{1}{N} \sum_{j=1}^N U_j e^{-i\vec{k} \cdot \vec{r}_j} = A e^{i\vec{k} \cdot \vec{r}_n}$$

$$n = 1, \dots, N$$

that is, when the data describe a single plane wave exactly.

The smaller $\epsilon(\vec{k})_{\min}$ is, in a given situation, the more likely is the hypothetical plane wave

$$A e^{i\vec{k} \cdot \vec{r}}$$

because the smaller $\epsilon(\vec{k})$ is, the larger the F-statistic is for the hypothesis. The F-statistic is given by

$$F = (N-1) \cdot P(\vec{k}) / \epsilon(\vec{k})$$

This single plane wave model is often applied in attempts to analyze a 2-signal case (or a possible 2-signal case). In such an analysis each signal is treated as if it existed by itself, the presence of the other being ignored with consequent distortion of estimates by mutual interference. This interference can be serious, and if the two signals are not separated in \vec{k} -space by at least the half-width of the main lobe of the array response, they are likely to appear as but one signal, their main lobes having coalesced. Attempts to improve the performance of the single wave hypothesis (in application to the two signal case) have been made in which the main lobe of the array response has been slenderized mathematically by alternative methods of esti-

mation of the wavenumber spectrum. The object has been to reduce the main-lobe half-width and so resolve signal pairs which otherwise have coalesced main-lobes indistinguishable from a signal case. These results have been marginal. In the various high-resolution techniques the influence of the one signal on the analysis of the other has been ignored.

Analysis of possible 2-signal cases calls for a 2-signal model, in particular when the 2-signals are known (or suspected) to be so close together as to have their main lobes merged.

As the 1-signal model serves for both the 0- and the 1-signal case, so one might expect a 2-signal model to be effective in all three cases: 0, 1, or 2-signals.

Multiple Signal Frequency-Wavenumber Analysis

By analogy to the 1-signal model, one would expect to solve a 2-signal model by minimizing the error

$$\epsilon = \sum_{n=1}^N \left| U_n - A e^{i\vec{k} \cdot \vec{r}_n} - B e^{i\vec{k} \cdot \vec{r}_n} \right|^2$$

varying $A, \vec{k}, B,$ and \vec{k} , where

B is the complex Fourier series term for the second hypothesized plane wave (at the same given frequency)

\vec{k} is the wavenumber of the hypothetical plane wave (at that same given frequency)

There are now two signals to solve for:

$$A e^{i\vec{k} \cdot \vec{r}_n} \quad \text{and} \quad B e^{i\vec{k} \cdot \vec{r}_n}$$

Let

$$T_n = U_n - A e^{i\vec{k} \cdot \vec{r}_n} - B e^{i\vec{k} \cdot \vec{r}_n}$$

then

$$\epsilon = \sum_{n=1}^N |T_n|^2 = \sum_{n=1}^N T_n^* T_n$$

Again, let

$$A = a + ic, \quad A^* = a - ic$$

Taking first partial derivatives while noting that

$$\frac{\partial A}{\partial a} = \frac{\partial A^*}{\partial a} = 1 \quad \text{and} \quad \frac{\partial A}{\partial c} = -\frac{\partial A^*}{\partial c} = i, \quad ,$$

$$\frac{\partial \epsilon}{\partial a} = \sum_{n=1}^N T_n^* (-e^{i\vec{k} \cdot \vec{r}_n}) + T_n (-e^{-i\vec{k} \cdot \vec{r}_n})$$

and

$$\frac{\partial \epsilon}{\partial c} = i \sum_{n=1}^N T_n^* (-e^{i\vec{k} \cdot \vec{r}_n}) + T_n (e^{-i\vec{k} \cdot \vec{r}_n})$$

Setting

$$\frac{\partial \epsilon}{\partial a} = \frac{\partial \epsilon}{\partial c} = 0$$

as in the 1-signal case,

$$\frac{\partial \epsilon}{\partial a} + i \frac{\partial \epsilon}{\partial c} = -2 \sum_{n=1}^N T_n e^{-i\vec{k} \cdot \vec{r}_n} = 0$$

Therefore,

$$A = \frac{1}{N} \sum_{n=1}^N (U_n - B e^{i\vec{k} \cdot \vec{r}_n}) \cdot e^{-i\vec{k} \cdot \vec{r}_n}$$

Analogously

$$B = \frac{1}{N} \sum_{n=1}^N (U_n - A e^{i\vec{k} \cdot \vec{r}_n}) \cdot e^{-i\vec{k} \cdot \vec{r}_n}$$

In this form A and B are optimized, that is, they produce the minimum value of ϵ for any arbitrary pair of \vec{k} and \vec{k} . Adopting the notation:

$$P \equiv \frac{1}{N} \sum_{n=1}^N U_n e^{-i\vec{k} \cdot \vec{r}_n}$$

$$Q \equiv \frac{1}{N} \sum_{n=1}^N U_n e^{-i\vec{k} \cdot \vec{r}_n}$$

$$E \equiv \frac{1}{N} \sum_{n=1}^N e^{i(\vec{k} - \vec{k}) \cdot \vec{r}_n}$$

one may write simply:

$$A = P - B \cdot E \quad \text{and} \quad B = Q - A \cdot E^*$$

Rearranging to solve A and B simultaneously

$$P = A + B \cdot E$$

$$Q = A \cdot E^* + B$$

$$A = \frac{\begin{vmatrix} P & E \\ Q & 1 \end{vmatrix}}{\begin{vmatrix} 1 & E \\ E^* & 1 \end{vmatrix}}, \quad B = \frac{\begin{vmatrix} 1 & P \\ E^* & Q \end{vmatrix}}{\begin{vmatrix} 1 & E \\ E^* & 1 \end{vmatrix}}$$

$$A = (P - QE) / (1 - E^*E)$$

$$B = (Q - PE^*) / (1 - E^*E)$$

Written out at length,

$$A = \frac{\frac{1}{N} \sum_{n=1}^N U_n e^{-i\vec{k} \cdot \vec{r}_n} - \frac{1}{N^2} \sum_{n=1}^N U_n e^{-i\vec{k} \cdot \vec{r}_n} \sum_{n=1}^N e^{i(\vec{k} - \vec{k}) \cdot \vec{r}_n}}{1 - \frac{1}{N} \sum_{n=1}^N e^{i(\vec{k} - \vec{k}) \cdot \vec{r}_n} \frac{1}{N} \sum_{j=1}^N e^{-i(\vec{k} - \vec{k}) \cdot \vec{r}_j}}$$

and B is similar in form.

Introducing a factor of $1/N$ into ϵ

$$\epsilon = \frac{1}{N} \sum_{n=1}^N T_n^* T_n$$

$$= \frac{1}{N} \sum_{n=1}^N (U_n^* - A^* e^{-i\vec{k} \cdot \vec{r}_n} - B^* e^{-i\vec{k} \cdot \vec{r}_n}) \times (U_n - A e^{i\vec{k} \cdot \vec{r}_n} - B e^{i\vec{k} \cdot \vec{r}_n})$$

$$\begin{aligned}
\epsilon &= \frac{1}{N} \sum_{\lambda=1}^N U_{\lambda}^* U_{\lambda} \\
&\quad - (A^* \frac{1}{N} \sum_{\lambda=1}^N U_{\lambda} e^{-i\vec{k} \cdot \vec{r}_{\lambda}} + A \frac{1}{N} \sum_{\lambda=1}^N U_{\lambda}^* e^{i\vec{k} \cdot \vec{r}_{\lambda}}) \\
&\quad - (B^* \frac{1}{N} \sum_{\lambda=1}^N U_{\lambda} e^{-i\vec{k} \cdot \vec{r}_{\lambda}} + B \frac{1}{N} \sum_{\lambda=1}^N U_{\lambda}^* e^{i\vec{k} \cdot \vec{r}_{\lambda}}) \\
&\quad + (A^* A + B^* B) \\
&\quad + (A^* B \frac{1}{N} \sum_{\lambda=1}^N e^{i(\vec{k} - \vec{k}') \cdot \vec{r}_{\lambda}} + AB^* \frac{1}{N} \sum_{\lambda=1}^N e^{-i(\vec{k} - \vec{k}') \cdot \vec{r}_{\lambda}})
\end{aligned}$$

$$\begin{aligned}
\epsilon &= \frac{1}{N} \sum_{\lambda=1}^N U_{\lambda}^* U_{\lambda} - (A^* P + AP^*) - (B^* Q + BQ^*) \\
&\quad + (A^* A + B^* B) + (A^* B E + AB^* E^*)
\end{aligned}$$

Rearranging the terms in ϵ ,

$$\begin{aligned}
\epsilon &= \frac{1}{N} \sum_{\lambda=1}^N U_{\lambda}^* U_{\lambda} - (A^* P + AP^*) - (B^* Q + BQ^*) \\
&\quad + A^*(A + BE) + B^*(AE^* + B)
\end{aligned}$$

and recalling that

$$P = A + BE \quad \text{and} \quad Q = AE^* + B$$

$$\epsilon = \frac{1}{N} \sum_{\lambda=1}^N U_{\lambda}^* U_{\lambda} - (AP^* + BQ^*)$$

Further, substituting

$$A = P - BE \quad \text{and} \quad B = Q - AE^*$$

$$\epsilon = \frac{1}{N} \sum_{\lambda=1}^N |U_{\lambda}|^2 - \frac{(P^*P + Q^*Q - PQ^*E^* - P^*QE)}{1 - E^*E}$$

or, written out,

$$\epsilon = \frac{1}{N} \sum_{\lambda=1}^N |U_{\lambda}|^2$$

$$\frac{-\frac{1}{N} \sum_{\lambda=1}^N \left| e^{i\vec{k} \cdot \vec{r}_{\lambda}} \frac{1}{N} \sum_{j=1}^N U_j e^{-i\vec{k} \cdot \vec{r}_j} - e^{i\vec{k} \cdot \vec{r}_{\lambda}} \frac{1}{N} \sum_{j=1}^N U_j e^{-i\vec{k} \cdot \vec{r}_j} \right|^2}{1 - \left| \frac{1}{N} \sum_{\lambda=1}^N e^{i(\vec{k} - \vec{k}) \cdot \vec{r}_{\lambda}} \right|^2}$$

The identity of these last 2 equations may be demonstrated

by noting that the numerator (above) equals

$$\begin{aligned} & \frac{1}{N} \sum_{\lambda=1}^N \left| e^{i\vec{k} \cdot \vec{r}_{\lambda}} P - e^{i\vec{k} \cdot \vec{r}_{\lambda}} Q \right|^2 \\ &= \frac{1}{N} \sum_{\lambda=1}^N \left(e^{-i\vec{k} \cdot \vec{r}_{\lambda}} P^* - e^{-i\vec{k} \cdot \vec{r}_{\lambda}} Q^* \right) \left(e^{i\vec{k} \cdot \vec{r}_{\lambda}} P - e^{i\vec{k} \cdot \vec{r}_{\lambda}} Q \right) \\ &= \frac{1}{N} \sum_{\lambda=1}^N \left\{ P^*P + Q^*Q - PQ^* e^{-i(\vec{k} - \vec{k}) \cdot \vec{r}_{\lambda}} - P^*Q e^{i(\vec{k} - \vec{k}) \cdot \vec{r}_{\lambda}} \right\} \\ &= P^*P + Q^*Q - PQ^*E^* - P^*QE \end{aligned}$$

Since ϵ is a sum of squares, by definition it must be non-negative everywhere. Therefore the second of the 2 terms in ϵ , above, must always be

$$\leq \frac{1}{N} \sum_{n=1}^N |U_n|^2$$

Thus to minimize \leftarrow , one must maximize

$$\frac{\frac{1}{N} \sum_{n=1}^N \left| e^{i\vec{k} \cdot \vec{r}_n} \cdot \frac{1}{N} \sum_{j=1}^N U_j e^{-i\vec{k} \cdot \vec{r}_j} - e^{i\vec{k} \cdot \vec{r}_n} \cdot \frac{1}{N} \sum_{j=1}^N U_j e^{-i\vec{k} \cdot \vec{r}_j} \right|^2}{\left| \frac{1}{N} \sum_{n=1}^N e^{i(\vec{k}-\vec{k}) \cdot \vec{r}_n} \right|^2}$$

This is the 2-signal test, analogous to the ordinary frequency-wavenumber spectrum, which is the 1-signal test. However, it is more convenient to retain the form

$$AP^* + BQ^*$$

This 2-signal $f-k$ "spectrum" then is computed from 3 beams (as the ordinary $f-k$ spectrum is computed from 1 beam).

The beams are

$$P = \frac{1}{N} \sum_{n=1}^N U_n e^{-i\vec{k} \cdot \vec{r}_n}$$

the mean of the data transforms that have been beamed to \vec{k} (one of the two wavenumber variables),

$$Q = \frac{1}{N} \sum_{n=1}^N U_n e^{-i\vec{k} \cdot \vec{r}_n}$$

the mean of the data transforms after beaming to \vec{k} (the other wavenumber variable),

$$E = \frac{1}{N} \sum_{n=1}^N e^{i(\vec{k}-\vec{k}) \cdot \vec{r}_n}$$

which is the (complex) array response

This 2-signal test is solved as is the ordinary $f-k$ spectrum, numerically, by searching the wavenumber space of

interest. Now, however, there are 4 dimensions to search, over which to test the error criterion.

It is instructive to submit a known pair of pure, noiseless signals to the 2-signal test to illustrate the function of the elements of the expression:

$$\text{Let } U_n = F e^{i\vec{k} \cdot \vec{r}_n} + G e^{i\vec{k}' \cdot \vec{r}_n}, \quad n=1, \dots, N$$

Beaming them exactly to \vec{k} and \vec{k}' (since these are known in this special case),

$$\begin{aligned} P &= \frac{1}{N} \sum_{n=1}^N (F e^{i\vec{k} \cdot \vec{r}_n} + G e^{i\vec{k}' \cdot \vec{r}_n}) \cdot e^{-i\vec{k} \cdot \vec{r}_n} \\ &= \frac{1}{N} \sum_{n=1}^N F + G e^{i(\vec{k}' - \vec{k}) \cdot \vec{r}_n} \\ &= F + G \cdot \frac{1}{N} \sum_{n=1}^N e^{i(\vec{k}' - \vec{k}) \cdot \vec{r}_n} = F + GE \end{aligned}$$

and

$$\begin{aligned} Q &= \frac{1}{N} \sum_{n=1}^N (F e^{i\vec{k} \cdot \vec{r}_n} + G e^{i\vec{k}' \cdot \vec{r}_n}) \cdot e^{-i\vec{k}' \cdot \vec{r}_n} \\ &= FE^* + G \end{aligned}$$

Then

$$\begin{aligned} A &= (P + QE) / (1 - E^*E) \\ &= (F + GE - (FE^* + G)E) / (1 - E^*E) \\ &= (F + GE - FE^*E - GE) / (1 - E^*E) \\ &= F(1 - E^*E) / (1 - E^*E) = F \end{aligned}$$

$$B = (FE^* + G - (F + GE)E^*) / (1 - E^*E)$$

$$B = G(1 - E^*E) / (1 - E^*E) = G$$

Thus

$$\begin{aligned} \epsilon &= \frac{1}{N} \sum_{n=1}^N \left| U_n - A e^{i\vec{k} \cdot \vec{r}_n} - B e^{i\vec{k} \cdot \vec{r}_n} \right|^2 \\ &= \frac{1}{N} \sum_{n=1}^N \left| F e^{i\vec{k} \cdot \vec{r}_n} + G e^{i\vec{k} \cdot \vec{r}_n} - F e^{i\vec{k} \cdot \vec{r}_n} - G e^{i\vec{k} \cdot \vec{r}_n} \right|^2 \end{aligned}$$

$$\epsilon = 0$$

This little exercise clarifies a bit the function of the array response, E , in the signal models A and B .

The development of the 2-signal test, of course, suggests the derivation of a 3-signal test, by analogy:

First, the form of the test would be, analogously,

$$\epsilon = \frac{1}{N} \sum_{n=1}^N \left| U_n - A e^{i\vec{k} \cdot \vec{r}_n} - B e^{i\vec{k} \cdot \vec{r}_n} - C e^{i\vec{k} \cdot \vec{r}_n} \right|^2$$

Introducing the notation

$$R \equiv \frac{1}{N} \sum_{n=1}^N U_n e^{-i\vec{k} \cdot \vec{r}_n} \quad E_1 \equiv \frac{1}{N} \sum_{n=1}^N e^{i(\vec{k} - \vec{k}) \cdot \vec{r}_n}$$

$$E_2 \equiv \frac{1}{N} \sum_{n=1}^N e^{i(\vec{k} - \vec{k}) \cdot \vec{r}_n} \quad E_3 \equiv \frac{1}{N} \sum_{n=1}^N e^{i(\vec{k} - \vec{k}) \cdot \vec{r}_n}$$

and expanding ϵ :

$$\begin{aligned} \epsilon &= \frac{1}{N} \sum_{n=1}^N \left(U_n^* - A^* e^{-i\vec{k} \cdot \vec{r}_n} - B^* e^{-i\vec{k} \cdot \vec{r}_n} - C^* e^{-i\vec{k} \cdot \vec{r}_n} \right) \\ &\quad \times \left(U_n - A e^{i\vec{k} \cdot \vec{r}_n} - B e^{i\vec{k} \cdot \vec{r}_n} - C e^{i\vec{k} \cdot \vec{r}_n} \right) \end{aligned}$$

$$\begin{aligned}
\llcorner &= \frac{1}{N} \sum_{\lambda=1}^N U_{\lambda}^* U_{\lambda} \\
&\quad - \left(A^* \frac{1}{N} \sum_{\lambda=1}^N U_{\lambda} e^{-i\vec{k} \cdot \vec{r}_{\lambda}} + A \frac{1}{N} \sum_{\lambda=1}^N U_{\lambda}^* e^{i\vec{k} \cdot \vec{r}_{\lambda}} \right) \\
&\quad - \left(B^* \frac{1}{N} \sum_{\lambda=1}^N U_{\lambda} e^{-i\vec{k} \cdot \vec{r}_{\lambda}} + B \frac{1}{N} \sum_{\lambda=1}^N U_{\lambda}^* e^{i\vec{k} \cdot \vec{r}_{\lambda}} \right) \\
&\quad - \left(C^* \frac{1}{N} \sum_{\lambda=1}^N U_{\lambda} e^{-i\vec{k} \cdot \vec{r}_{\lambda}} + C \frac{1}{N} \sum_{\lambda=1}^N U_{\lambda}^* e^{i\vec{k} \cdot \vec{r}_{\lambda}} \right) \\
&\quad + (A^*A + B^*B + C^*C) \\
&\quad + \left(A^*B \frac{1}{N} \sum_{\lambda=1}^N e^{i(\vec{k}-\vec{k}) \cdot \vec{r}_{\lambda}} + AB^* \frac{1}{N} \sum_{\lambda=1}^N e^{-i(\vec{k}-\vec{k}) \cdot \vec{r}_{\lambda}} \right) \\
&\quad + \left(B^*C \frac{1}{N} \sum_{\lambda=1}^N e^{i(\vec{k}-\vec{k}) \cdot \vec{r}_{\lambda}} + BC^* \frac{1}{N} \sum_{\lambda=1}^N e^{-i(\vec{k}-\vec{k}) \cdot \vec{r}_{\lambda}} \right) \\
&\quad + \left(A^*C \frac{1}{N} \sum_{\lambda=1}^N e^{i(\vec{k}-\vec{k}) \cdot \vec{r}_{\lambda}} + AC^* \frac{1}{N} \sum_{\lambda=1}^N e^{-i(\vec{k}-\vec{k}) \cdot \vec{r}_{\lambda}} \right)
\end{aligned}$$

$$\begin{aligned}
\llcorner &= \frac{1}{N} \sum_{\lambda=1}^N U_{\lambda}^* U_{\lambda} \\
&\quad - (A^*P + AP^*) - (B^*Q + BQ^*) - (C^*R + CR^*) \\
&\quad + (A^*A + B^*B + C^*C) \\
&\quad + (A^*BE_1 + AB^*E_1^*) + (B^*CE_3 + BC^*E_3^*) + (A^*CE_2 + AC^*E_2^*)
\end{aligned}$$

Now noting that in the 2-signal test

$$P = A + BE \quad \text{and}$$

$$Q = AE^* + B$$

so that

$$A = \frac{\begin{vmatrix} P & E \\ Q & 1 \end{vmatrix}}{\begin{vmatrix} 1 & E \\ E^* & 1 \end{vmatrix}} \quad B = \frac{\begin{vmatrix} 1 & P \\ E^* & Q \end{vmatrix}}{\begin{vmatrix} 1 & E \\ E^* & 1 \end{vmatrix}}$$

one recognizes that, in the 3-signal test,

$$P = A + BE_1 + CE_2$$

$$Q = AE_1^* + B + CE_3$$

$$R = AE_2^* + BE_3^* + C$$

and, defining

$$\text{den} \equiv \begin{vmatrix} 1 & E_1 & E_2 \\ E_1^* & 1 & E_3 \\ E_2^* & E_3^* & 1 \end{vmatrix}$$

$$A = \begin{vmatrix} P & E_1 & E_2 \\ Q & 1 & E_3 \\ R & E_3^* & 1 \end{vmatrix} \cdot \text{den}^{-1} \quad , \text{ etc.}, \text{ or}$$

$$A = [P(1 - E_3^*E_3) + Q(E_3^*E_2 - E_1) + R(E_1E_3 - E_2)]/\text{den}$$

$$B = [P(E_2^*E_3 - E_1^*) + Q(1 - E_2^*E_2) + R(E_1^*E_2 - E_3)]/\text{den}$$

$$C = [P(E_1^*E_3^* - E_2^*) + Q(E_1E_2^* - E_3^*) + R(1 - E_1^*E_1)]/\text{den}$$

$$\text{den} = 1 - E_1^*E_1 - E_2^*E_2 - E_3^*E_3 + E_1E_2^*E_3 + E_1^*E_2E_3^*$$

Now rearranging ϵ ,

$$\epsilon = \frac{1}{N} \sum_{\lambda=1}^N U_{\lambda}^* U_{\lambda} - (A^*P + B^*Q + C^*R) - (AP^* + BQ^* + CR^*)$$

$$+ A^*(A + BE_1 + CE_2) + B^*(AE_1^* + B + CE_3) + C^*(AE_2^* + BE_3^* + C)$$

and substituting P , Q , and R

$$\epsilon = \frac{1}{N} \sum_{\lambda=1}^N U_{\lambda}^* U_{\lambda} - (AP^* + BQ^* + CR^*)$$

To minimize ϵ , then, one will maximize

$$AP^* + BQ^* + CR^*$$

the 3-signal test, or 3-signal analog to the conventional, 1-signal frequency-wavenumber spectrum. The function is composed of 6 beams: P , Q , and R , the 3 beams of the data, U_{λ} , and E_1 , E_2 , and E_3 , the 3 beams of the array response.

Remembering the 1-signal test (conventional f - k spectrum),

$$\begin{aligned} \frac{1}{N} \epsilon &= \frac{1}{N} \sum_{\lambda=1}^N |U_{\lambda} - A e^{i\vec{k} \cdot \vec{r}_{\lambda}}|^2 \\ &= \frac{1}{N} \sum_{\lambda=1}^N (U_{\lambda}^* - A^* e^{-i\vec{k} \cdot \vec{r}_{\lambda}})(U_{\lambda} - A e^{i\vec{k} \cdot \vec{r}_{\lambda}}) \end{aligned}$$

we may rewrite it as

$$\frac{1}{N} \epsilon = \frac{1}{N} \sum_{\lambda=1}^N U_{\lambda}^* U_{\lambda} - A^*P - AP^* - A^*A$$

(since $P = \frac{1}{N} \sum_{n=1}^N U_n e^{i\vec{k} \cdot \vec{r}_n}$), or

$$\begin{aligned} \frac{1}{N} \epsilon &= \frac{1}{N} \sum_{n=1}^N U_n^* U_n - A^* A - AP^* + A^* A \\ &= \frac{1}{N} \sum_{n=1}^N U_n^* U_n - AP^* \end{aligned}$$

Thus

$$AP^* = \frac{1}{N} \left(\frac{1}{N} \left| \sum_{n=1}^N U_n e^{i\vec{k} \cdot \vec{r}_n} \right|^2 \right)$$

is the expression one must maximize in order to minimize the error. So the f - k spectrum (for the 1-signal, conventional, case) is

$$AP^*,$$

and

$$AP^* + BQ^* \text{ is the 2-signal test,}$$

and

$$AP^* + BQ^* + CR^* \text{ is the 3-signal test.}$$

In the 1-signal test

$$A = \frac{P}{1}$$

For the 2-signal test

$$A = \frac{\begin{vmatrix} P & E_1 \\ Q & 1 \end{vmatrix}}{\begin{vmatrix} 1 & E_1 \\ E_1^* & 1 \end{vmatrix}}, \quad B = \frac{\begin{vmatrix} 1 & P \\ E_1^* & Q \end{vmatrix}}{\begin{vmatrix} 1 & E_1 \\ E_1^* & 1 \end{vmatrix}}$$

For the 3-signal test

$$A = \frac{\begin{vmatrix} P & E_1 & E_2 \\ Q & 1 & E_3 \\ R & E_3^* & 1 \end{vmatrix}}{\begin{vmatrix} 1 & E_1 & E_2 \\ E_1^* & 1 & E_3 \\ E_2^* & E_3^* & 1 \end{vmatrix}}, \text{ etc.}$$

This formalism makes evident the relationship between the successive tests. Thus one may extropolate and directly write the expression for the M-signal test in simple, terse form. For example, the 4-signal test is

$$AP^* + BQ^* + CR^* + DS^*$$

in which S , the sum of the data beamed to yet a 4th point \vec{k} , is introduced into the sequence P, Q , and R ;

and in which

$$A = \frac{\begin{vmatrix} P & E_1 & E_2 & E_4 \\ Q & I & E_3 & E_5 \\ R & E_3^* & I & E_6 \\ S & E_5^* & E_6^* & I \end{vmatrix}}{\begin{vmatrix} I & E_1 & E_2 & E_4 \\ E_1 & I & E_3 & E_5 \\ E_2^* & E_3^* & I & E_6 \\ E_4^* & E_5^* & E_6^* & I \end{vmatrix}}, \text{ etc.,}$$

and E_1 is the array response at $(\vec{k}-\vec{k})$, E_5 , that at $(\vec{k}-\vec{k})$, etc.

Note that the four-signal test is computed from 10 beams; 4 beams of the input, U_n , and 6 of the array response. In general, the M-signal test requires M beams of input data (U_n), and $M(M-1)/2$ beams on the array response, for a

total of $M(M+1)/2$ beams to compute the least-squares error at any point in the $2M$ -dimensional space. But the beams on the array response are computed from the same complex trigonometric terms that are required for the M beams of the input data. So the M -signal test requires evaluation of $2MN$ sine and cosine terms to compute the error at any point (N is the number of sensors in the array). Thus the number of trigonometric terms requiring computation increases linearly with M .

It must be noted that a multiple signal test is not everywhere well-behaved, but has a singularity. For example, in the case of the 2-signal test, if

$$\vec{k} \rightarrow \vec{k}$$

so that

$$Q \rightarrow P$$

and

$$E \rightarrow 1$$

\in is undefined. The value it will take on at $\vec{k} = \vec{k}$ depends on the direction from which $\vec{k} \rightarrow \vec{k}$. Though this can, of course, be shown analytically, it is a bit tedious for repetition here. The contoured map of an example (figure 1) displays this characteristic graphically. The contoured function is the 2-signal test

$$AP^* + BQ^*$$

with \vec{k} held fixed as \vec{k} varies over the plane. Note that the contour lines all run together at $\vec{k} = \vec{k}$. \vec{k} may range arbitrarily close to \vec{k} but must not take on that value exactly. The data in this figure consist of 2 closely spaced signals. The fixed vector, \vec{k} , was set at the peak of their merged main lobes.

One might dismiss this singularity from practical consideration since signals of identical speed and bearing are indistinguishable by array methods. The test for 2 signals at the same wavenumber location is thus unnecessary anyway. But if the 2-signal test, say, is applied to data composed of only 1 signal, must not both the probe vectors approach the same point, i.e., the wavenumber location of the input signal, in order to merge and reduce the function to the 1-signal test? We have seen that when the data, U_λ , consist of the same number of signals as that for which one is testing, the test performs as expected: the error is minimized at the wavenumber location of those input signals, and the signals are recovered undistorted. Suppose, though, that the 2-signal test, say, is applied to data consisting of just plane wave. Let

$$U_\lambda = F e^{i\vec{k} \cdot \vec{r}_\lambda} .$$

$$T_\lambda = U_\lambda - A e^{i\vec{k} \cdot \vec{r}_\lambda} - B e^{i\vec{k} \cdot \vec{r}_\lambda}$$

in the error expression

$$\epsilon = \frac{1}{N} \sum_{\lambda=1}^N |T_{\lambda}|^2$$

We have to maximize

$$AP^* + BQ^*$$

$$P = F \frac{1}{N} \sum_{\lambda=1}^N e^{i(\bar{k}-\bar{k}) \cdot \bar{r}_{\lambda}}, \text{ and } Q = F \frac{1}{N} \sum_{\lambda=1}^N e^{i(\bar{k}-\bar{k}) \cdot \bar{r}_{\lambda}}$$

If \bar{k} goes to \bar{k} , then

$$P = F, \quad Q = FE^*$$

and

$$A = (P - QE) / (1 - E^*E)$$

becomes

$$A = (F - FE^*E) / (1 - E^*E) = F$$

and

$$B = (Q - PE^*) / (1 - E^*E) = (FE^* - FE^*) / (1 - E^*E) = 0$$

and

$$\begin{aligned} \epsilon &= \frac{1}{N} \sum_{\lambda=1}^N U_{\lambda}^* U_{\lambda} - (AP^* + BQ^*) \\ &= \frac{1}{N} \sum_{\lambda=1}^N (F^* e^{-i\bar{k} \cdot \bar{r}_{\lambda}}) (F e^{i\bar{k} \cdot \bar{r}_{\lambda}}) - (F^* F + 0) \\ &= \frac{1}{N} \sum_{\lambda=1}^N F^* F - F^* F = 0 \end{aligned}$$

When \bar{k} goes to \bar{k} the error is minimized, the signal, F , is recovered undistorted, and the hypothesized second signal vanishes. This solution is invariant though

\vec{k} be permitted to range over the entire k -plane, excepting the point \vec{k} . Thus the 2-signal test does not reduce to the ordinary f - k spectrum in the presence of a single plane wave, and \vec{k} is not required to go to \vec{k} nor would the gradient of ϵ with respect to \vec{k} lead to \vec{k} (if one were using a steepest descent technique to minimize ϵ).

Numerical Solution of the Multiple Signal Test

One might propose to carry out the numerical solution of a multiple signal test by a straightforward search of the entire wavenumber space of interest, as is done in the computation of the conventional f - k spectrum. But the multiple signal test may be used in more practical fashion, with greater efficiency, as a follow-up to the ordinary f - k spectrum. Since a high-resolution array process by design is intended to separate signals otherwise unresolvable, there is sound justification to limit its use to the vicinity of signals tentatively identified beforehand by less powerful but faster techniques. This is an advantageous circumstance, since an M -signal test is a function of $2M$ dimensions of wavenumber and would otherwise prove computationally less efficient. Applying the 2 - signal test to the highest peak of an ordinary f - k spectrum, then, one hypothesizes the presence of 2 plane waves which appear as only 1 because of their proximity. By the hypothesis the spectral peak lies within the area of the main lobe of either signal and thus ϵ may be minimized directly by

the method of steepest descent. This is the procedure used here.

Since, as has been shown earlier,

$$\vec{k} = \bar{k}$$

is prohibited, the descent cannot begin from any one single point in the \bar{k} -plane, as, for example, the peak under consideration. But any pair of points in that vicinity is suitable; all lead to the same solution. A convenient pair are (1) the peak, and (2) the adjacent minimum of ϵ with respect to, say, \vec{k} when \bar{k} is fixed at the peak as in the previously discussed figure 1. The gradient of ϵ is computed at this pair and ϵ itself then recomputed at a new location down the gradient. The length of this first step in the descent is some fraction of the width of the array-response main-lobe, thus chosen to ensure that the process does not jump from the vicinity of the solution into the range of an adjacent relative minimum. The gradient is newly computed at this second location; another somewhat smaller step is taken down the gradient; the gradient is once more computed, now at this third location, and so forth in successively smaller steps until the point is reached in that 4-dimensional space at which the gradient goes to zero.

Some examples with synthetic data for the LASA LP array follow.

Figure 2 represents the array response of LASA. The function is mapped in contours of 3 db intervals down from the peak at the center. At present 7 long-period vertical seismometers remain at LASA: the D-ring, 2 elements of the C-ring, and the center sensor at A0. Thus, the half-width of the main lobe is about 0.016 cycle/km. At 20 seconds period and 3.5 km/sec that half-width intercepts nearly 70 degrees of azimuth.

Since the error expression for the 2-signal test is a function of 4 dimensions of wavenumber and cannot be presented in map form as are ordinary f-k spectral sections, numerical presentations must be resorted to. Figure 3 presents the first and last page of computer print-out of the successive steps in the solution of a single-frequency test case of 2 noiseless signals separated by 1/8 of the array main-lobe half-width. One signal is 2 magnitudes greater than the other (ten times the amplitude) and is 180° out of phase with it at the array center such that they destructively interfere with each other. At the upper right of the first page are the signal descriptions; beneath that are the array coordinates (in km.) and the Fourier transforms of the signals. Thereafter each successive line represents a step in the

optimization. The E format number at the left in each line is the error term. The amplitude, phase and coordinates (kx, ky) at each pair of points are given in the two columns enclosed by vertical lines. The unit vector of the gradient is given by the 4 numbers at the right of the page. The size of the step from the previous point just precedes the unit vector.

The solution is given at the bottom of the second page by the complex transforms, wavenumber locations and the final error value. The solution is both accurate and precise; the high resolution has introduced no distortion such as characterizes the non-linear techniques.

The computer routines of figure 3 that apply the 2-signal test were introduced into a general f-k analysis program called FKSCAN which was styled after FKCOMB [Mack and Smart (24)]. To this automated high-resolution processor synthetic time series were submitted for trial analysis. One test consisted of a unit plane-wave from 356° at 3.5 km/s to which synthetic random noise was added to make the signal-to-noise power ratio equal to 4. To this combination was added a second plane-wave, 2 magnitudes larger than the first, from 302° , also at 3.5 km/s. In the band of interest (6-23 seconds period) the 2 signals overlap in wavenumber space. At 23.3 seconds period they are separated by 0.7 the main-lobe half-

width; at 16.0 seconds, by 1.0. Each signal was of 20 seconds period enclosed in 192 second cosine envelope. They arrive at the array center at the same instant. A 256-second time window was applied for the analysis. The resulting bulletin from FKSCAN is given in figure 4, and is self-explanatory. The larger signal is shown arriving from 301° at 3.518 km/s; the smaller from 354° at 3.059 km/s. They differ in apparent magnitude by 2.05 (from the ratio of the power summed over the band).

The last item on the second page gives a measure of the assurance one would have had of the validity of such a detection had it appeared in processing of real data. In routine processing of such 4 minute, 16 second windows each interval yields 2 suits of vectors, or detections. At the rate of 2 suits of random vectors per time interval, so anomalous an angular concentration of vectors would appear only once every 11 days, on the average. [This algorithm, installed in FKSCAN to provide an independent detection statistic separate from the F-statistic, is based on a probability expression developed by the author which he intends subsequently to submit for publication.]

Thus, in this modest test of the 2-signal detector functioning in the presence of random noise, the small, "hidden" signal is recovered as a strong detection.

The array, the relative magnitudes and azimuthal spacing of these 2 test signals, and the frequency band in which the search was made anticipate a test on real LASA data in which similar conditions were expected. The 2 seismic events sought in the real data are recorded in the U.S. Department of the Interior's Earthquake Data Reports 36-74 and 43-74. On 31 May 74 at 0313:11 an earthquake occurred in the vicinity of Unimak Island in the Aleutians. At 0326:57 a second event occurred in eastern Kazakh SSR. The first quake had a body wave magnitude of 4.8 and a surface wave magnitude of 4.6. The second event was recorded as M_B 5.9, with M_S measurements unavailable. The Unimak signal was expected at LASA about 0330 from 302° , with the Kazakh signal expected about 0406, in the ongoing coda, from 356° . Figure 5 displays the seismograms of this interval for all seven LASA stations. The figure begins at 0329:08 and continues past 0415. The anticipated onset of the Kazakh surface wave is marked by the arrow at 0406:09. The circled numerals at the bottom of the figure number the successive time windows, indicated by arrows, that were submitted to the high-resolution array processor.

Figures 6 through 11 are the resulting bulletins for the 6 time-windows marked on the seismograms. The relatively narrow band from 16-23 seconds period was chosen for this analysis because it was anticipated that the faint signal from

from Kazakh was most likely to appear in these frequencies if at all. As before there are two sets of tentative detections in each time-window, that is, 2 detections per frequency. The suit at the upper left contains, at each frequency, the signal pick of greatest power. One might call these the primary detections. The suit at the upper right contains the smaller signal picks. Before each suit is submitted to azimuthal distribution analysis, the program computes the straight line through the frequency-wavenumber origin $(0,0,0)$ which, in the least squares sense, best fits all the vectors in the suit. The back azimuth and phase velocity of that mean are then printed in the bulletin.

The back-azimuth of the mean of the primary signal picks in succeeding time-windows, then, for these 6 intervals reads, in sequence: 328° , 319° , 323° , 353° , 356° , and 318° . In windows 1, 2, and 3 the detector is "triggering" on the ongoing coda from the Unimak earthquake. But in windows 4 and 5 it turns and indicates the back azimuth of the Kazakh site. Then in window 6 it returns to the Unimak coda.

Figures 12 and 17 (one for each of these 6 time-windows) are contoured plots in 3 db intervals, of the conventional wavenumber spectra, integrated over the frequency band 0.043-0.063 Hz (16-23 seconds period) after the secondary detections derived from the high-resolution processor have been filtered

out. These spectra make visible the observations of the previous paragraph.

Conclusions

The high resolving power of the linear multiple-signal analysis and the fidelity of its estimates have been demonstrated by computer examples and by application to real signals.

Computer examples indicate that this technique is capable, in the absence of noise, of exactly recovering the amplitude, phase, and velocity of two simultaneously arriving Rayleigh waves at, for example, LASA, which differ in azimuth by as little as 8° , even if one signal is 10 times larger than the other. In the case of the simultaneous arrival of a small signal with S/N of 2 and a signal 100 times larger, with a difference in azimuth between the two of 54° , the magnitude (M_s) of the small signal can be recovered with less than 3% distortion.

The extraction of the Rayleigh wave arriving from a nuclear test in Kazakh from the coda of an Aleutian earthquake demonstrates the practical application of the technique. It should now be possible to utilize long period array data to obtain accurate amplitude and phase information for small events which were previously "hidden" in the coda of much larger events. In addition, the linear multiple signal estimator should make possible the decomposition of large

surface waves into primary and multipath components on the basis of differences in arrival azimuth. Better estimates of the true amplitude and phase will result by removal of the multipath effects, and the spectrum and angle of approach of the multipath components will provide information as to the location and nature of the conditions which give rise to multipaths.

FIGURES

1. A contoured map of a 2-signal test of synthetic data with one probe point held fixed while the other ranges over the wavenumber plane 39
2. The array response of the 7-element long-period vertical seismic array at LASA 40
3. The successive steps in a 2-signal analysis . . 41 & 42
4. The bulletin from the high-resolution frequency-wavenumber processor for synthetic LASA data 43 & 44
5. Seismograms from the LASA LP array. 0329:08 through 0415 GMT, 31MAY74. 45
6. High-resolution analysis; 0349:05 to 0353:20 GMT, 31MAY74, LASA LP array 46
7. High-resolution analysis; 0353:21 to 0357:36 GMT, 31MAY74, LASA LP array 47
8. High-resolution analysis; 0357:37 to 0401:52 GMT, 31MAY74, LASA LP array 48
9. High-resolution analysis; 0401:53 to 0406:08 GMT, 31MAY74, LASA LP array 49
10. High-resolution analysis; 0406:09 to 0410:24 GMT, 31MAY74, LASA LP array 50
11. High-resolution analysis; 0410:25 to 0414:40 GMT, 31MAY74, LASA LP array 51
12. Filtered wavenumber spectrum for interval 1, 31MAY74, LASA LP array . . . 52
13. Filtered wavenumber spectrum for interval 2, 31MAY74, LASA LP array . . . 53

14. Filtered wavenumber spectrum for interval 3,
31MAY74, LASA LP array . . . 54
15. Filtered wavenumber spectrum for interval 4,
31MAY74, LASA LP array . . . 55
16. Filtered wavenumber spectrum for interval 5,
31MAY74, LASA LP array . . . 56
17. Filtered wavenumber spectrum for interval 6,
31MAY74, LASA LP array . . . 57

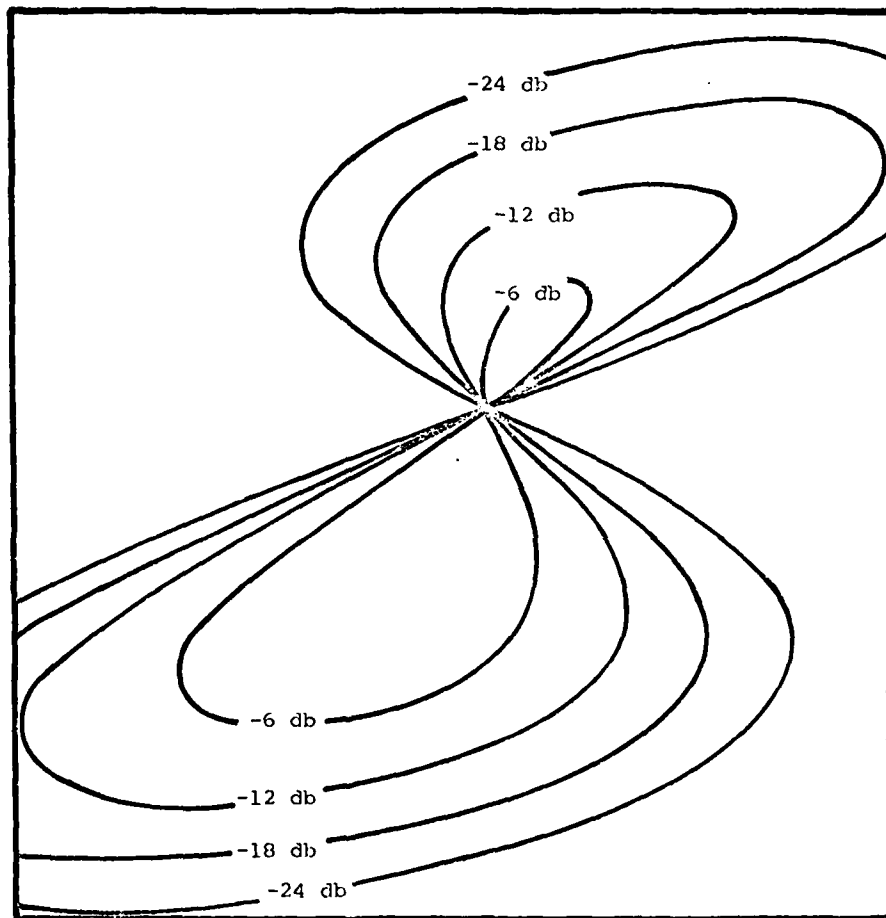


Figure 1. A contoured map of a 2-signal test of synthetic data (see page 27) with one probe point held fixed while the other ranges over the wavenumber plane. When both probes occupy the same point the function is ambiguous, its value varying with the direction from which one probe approaches the other. Note the intersection of the contours.

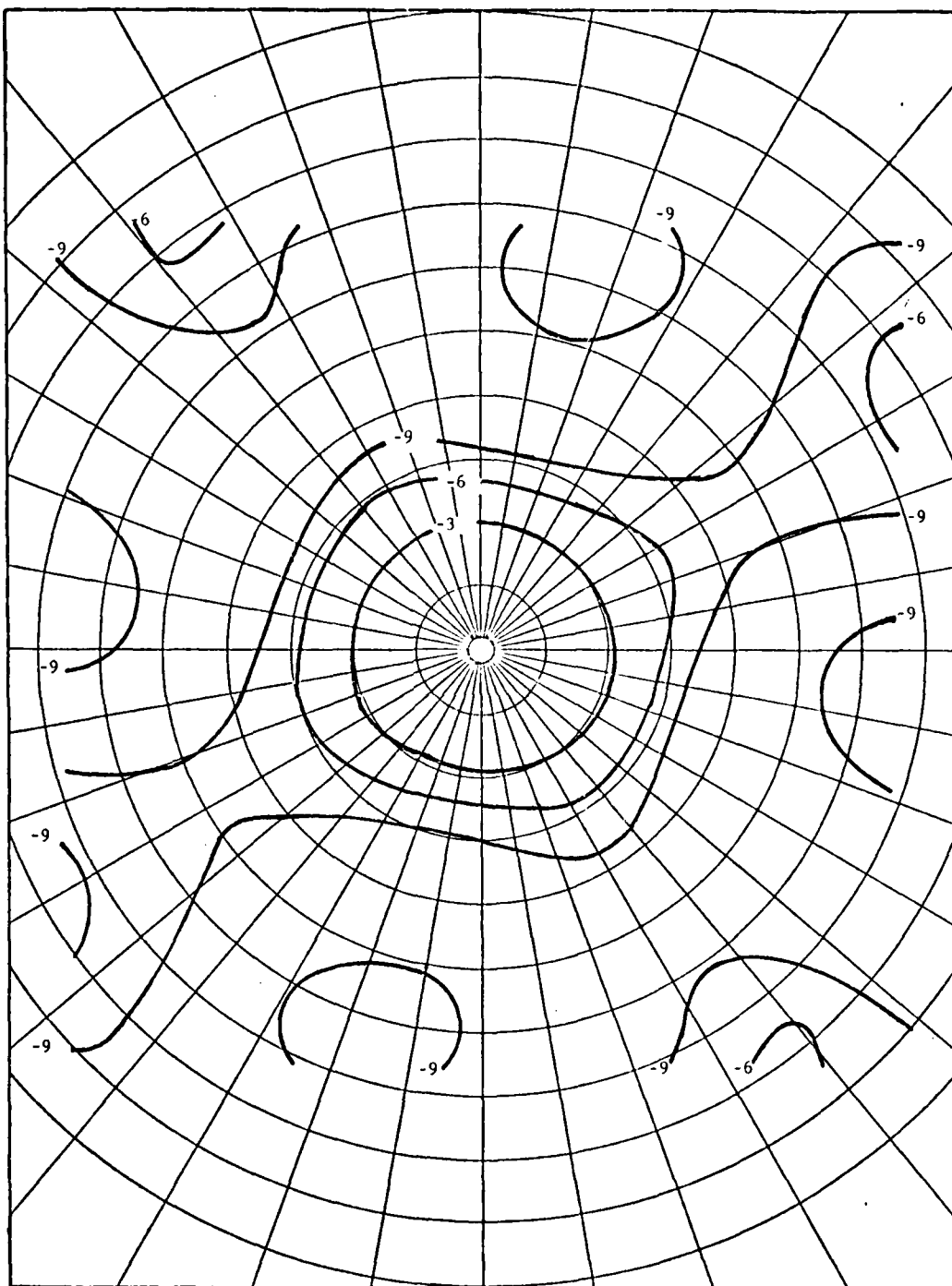


Figure 2. The array response of the 7-element long-period vertical seismic array at LASA. The contour interval is in 3 db steps. The scale is 0.01 cycle/km per inch.

NSETS = 7 BASE = .000 JUMP = .0 PHASE2 = 10.0
 LUTIC = 1 FACTRY = 4.000 LAUNCH = 30 SIZE1 = 1.00
 LUTP = 1 RD = .100 SLACK = .000 WAVE1 = .00100
 BREAK = 5.0 BU = .000 HNIC = .990 WAVE2 = .00000

PROGRAM 2-4 FK VERSION DATED 16APR76 EUGENE SMART

THE SEARCH WILL ORIGINATE AT [XX = .0000, KY = .0000]. THE INITIAL RANDOM NUMBER IS 4647. AND THE NUMBER OF SETS IS 0

STOMA_173-NSISE RATIO = .1000E 30

BELG. ARE LISTED THE FOURIER TRANSFORMS OF THE 2 SIGNALS
 SIGNAL ONE SIGNAL TWO

REAL	IMAGINARY	REAL	IMAGINARY
.99999999999999	.00000000000000	.00000000000000	.00000000000000
.997348726766	.072773304482	.072773304482	.997348726766
.959512286068	.013244557373	.013244557373	.959512286068
.93277331448	.02332230007	.02332230007	.93277331448
.9073112849	.07639953283	.07639953283	.9073112849
.8730603412	.1582943258	.1582943258	.8730603412
.8407272356	.3117443238	.3117443238	.8407272356
.8111111111	.0000000000	.0000000000	.8111111111
.7841111111	.0000000000	.0000000000	.7841111111
.7591111111	.0000000000	.0000000000	.7591111111
.7361111111	.0000000000	.0000000000	.7361111111
.7151111111	.0000000000	.0000000000	.7151111111
.6961111111	.0000000000	.0000000000	.6961111111
.6791111111	.0000000000	.0000000000	.6791111111
.6641111111	.0000000000	.0000000000	.6641111111
.6511111111	.0000000000	.0000000000	.6511111111
.6401111111	.0000000000	.0000000000	.6401111111
.6311111111	.0000000000	.0000000000	.6311111111
.6241111111	.0000000000	.0000000000	.6241111111
.6191111111	.0000000000	.0000000000	.6191111111
.6161111111	.0000000000	.0000000000	.6161111111
.6151111111	.0000000000	.0000000000	.6151111111
.6161111111	.0000000000	.0000000000	.6161111111
.6191111111	.0000000000	.0000000000	.6191111111
.6241111111	.0000000000	.0000000000	.6241111111
.6311111111	.0000000000	.0000000000	.6311111111
.6401111111	.0000000000	.0000000000	.6401111111
.6511111111	.0000000000	.0000000000	.6511111111
.6641111111	.0000000000	.0000000000	.6641111111
.6791111111	.0000000000	.0000000000	.6791111111
.6961111111	.0000000000	.0000000000	.6961111111
.7151111111	.0000000000	.0000000000	.7151111111
.7361111111	.0000000000	.0000000000	.7361111111
.7591111111	.0000000000	.0000000000	.7591111111
.7841111111	.0000000000	.0000000000	.7841111111
.8111111111	.0000000000	.0000000000	.8111111111
.8407272356	.3117443238	.3117443238	.8407272356
.8730603412	.1582943258	.1582943258	.8730603412
.9073112849	.07639953283	.07639953283	.9073112849
.93277331448	.02332230007	.02332230007	.93277331448
.959512286068	.013244557373	.013244557373	.959512286068
.997348726766	.072773304482	.072773304482	.997348726766
.99999999999999	.00000000000000	.00000000000000	.99999999999999

Figure 3. The successive steps in 2-signal analysis. See p 33.

THE FOLLOWING BULLETIN PRESENTS THE RESULTS OF HIGH RESOLUTION FREQUENCY-AWENUMBER ANALYSIS APPLIED TO THE DATA OF THE PRECEDING TIME INTERVAL.

PERIOD SECONDS	APPARENT PHASE IN K/M/S	BACK AZIMUTH IN DEGREES		POWER	F-STATISTIC	PERIOD IN SECONDS	APPARENT PHASE IN K/M/S	BACK AZIMUTH IN DEGREES		POWER	F-STATISTIC
		EAST OF NORTH	NORTH					EAST OF NORTH	NORTH		
23.273	3.555	303	524E-02	10707	23.273	2.443	94	326E-04	57		
21.333	3.379	302	484E-01	12279	21.333	2.160	14	257E-03	53		
19.592	3.565	302	735E-01	11499	19.592	2.534	350	777E-03	114		
18.245	3.565	302	237E-01	5333	18.286	2.921	14	336E-03	53		
17.267	3.528	314	628E-03	7431	17.067	3.215	339	172E-04	233		
16.200	3.337	304	455E-04	3552	16.000	4.524	345	115E-05	53		

THERE ARE 6 VECTORS AT THE LEFT, ABOVE, HAVING F-STATISTICS GREATER THAN $^{\circ}C$. THERE ARE 6 VECTORS AT THE RIGHT, ABOVE, HAVING F-STATISTICS GREATER THAN $^{\circ}C$.
A LEAST SQUARES FIT OF ALL 6 AWENUMBER VECTORS TO A CONSTANT VELOCITY-AZIMUTH LINE THROUGH F-K SPACE YIELDED AN APPARENT PHASE VELOCITY OF 3.531 K/M/S AT 301 DEGREES, WITH AN RMS ERROR TO THE FIT OF .000 CYCLES/KM.

THE FOLLOWING LIST REPEATS, IN AZIMUTHAL ORDER, ALL THE ABOVE VECTORS AT THE LEFT HAVING F-STATISTICS GREATER THAN $^{\circ}C$. FOR EACH VECTOR THE LAST COLUMN GIVES, IN DEGREES, THE DISTANCE FROM THE PRECEDING VECTOR.

AZIMUTH	SPEED	F-STAT	PERIOD	DEGREES
301	3.422	7431	17.07	357.4
301	3.399	3342	16.00	.2
302	3.532	12089	19.65	1.0
302	3.555	5333	19.80	.2
302	3.379	12279	21.33	.4
303	3.635	10707	23.27	.5

THE MOST ANOMALOUS CONCENTRATION OF VECTORS IN THE ABOVE LIST OF 6 IS THAT OF THE GROUP OF 3 VECTORS BETWEEN 301 AND 302 DEGREES. THE ELEMENT OF 5 OR MORE OUT OF 6 VECTORS WITHIN 1.8 DEGREES OR LESS WILL OCCUR AT RANDOM BY THE AVERAGE OF EACH EVERY 1684.08 DAYS.
A LEAST SQUARES FIT OF ALL 6 AWENUMBER VECTORS TO A CONSTANT VELOCITY-AZIMUTH LINE THROUGH F-K SPACE YIELDED AN APPARENT PHASE VELOCITY OF 3.452 K/M/S AT 301 DEGREES, WITH AN RMS ERROR TO THE FIT OF .000 CYCLES/KM.

THERE ARE 6 VECTORS AT THE RIGHT, ABOVE, HAVING F-STATISTICS GREATER THAN $^{\circ}C$.
A LEAST SQUARES FIT OF ALL 6 AWENUMBER VECTORS TO A CONSTANT VELOCITY-AZIMUTH LINE THROUGH F-K SPACE YIELDED AN APPARENT PHASE VELOCITY OF 3.555 K/M/S AT 304 DEGREES, WITH AN RMS ERROR TO THE FIT OF .005 CYCLES/KM.

Figure 4a. The bulletin from the high-resolution frequency-wavenumber processor for synthetic LASA data: a signal from 356° at 3.5 km/s with S/N equal to 4, plus a signal from 302° at 3.5 km/s which is 2 magnitudes larger. See p. 34.

THE FOLLOWING LIST REPEATS, IN AZIMUTH ORDER, ALL THE ABOVE VECTORS AT THE RIGHT HAVING F-STATISTICS GREATER THAN .05 FOR EACH VECTOR THE LAST COLUMN GIVES, IN DEGREES, THE DISTANCE FROM THE PRECEDING VECTOR.

	AZIMUTH	SPEED	F-STAT	PERIOD	DEGREES
1	24164	53	21.39	11.3	
2	24521	83	18.25	8.8	
3	24443	67	23.27	7.7	
339	34215	203	17.57	32.4	
345	44524	93	16.00	5.3	
350	24334	113	13.69	4.3	

THE MOST ANOMALOUS CONCENTRATION OF VECTORS IN THE ABOVE LIST OF 6 IS THAT OF THE GROUP OF 4 VECTORS BETWEEN 339 AND 345 DEGREES. THE EQUIVALENT OF 6 OR MORE BUT OF 6 VECTORS WITHIN 30.6 DEGREES OR LESS WILL OCCUR AT RANDOM ON THE AVERAGE OF ONCE EVERY 11.3 DAYS. AVERAGE VECTOR TO A CONSTANT VELOCITY-AZIMUTH LINE THROUGH F-K SPACE YIELDED AN APPARENT PHASE VELOCITY OF 3.053 X/MS AT 354 DEGREES, WITH AN RMS ERROR TO THE FIT OF .005 CYCLES/KM.

Figure 4b: A continuation from the previous page.

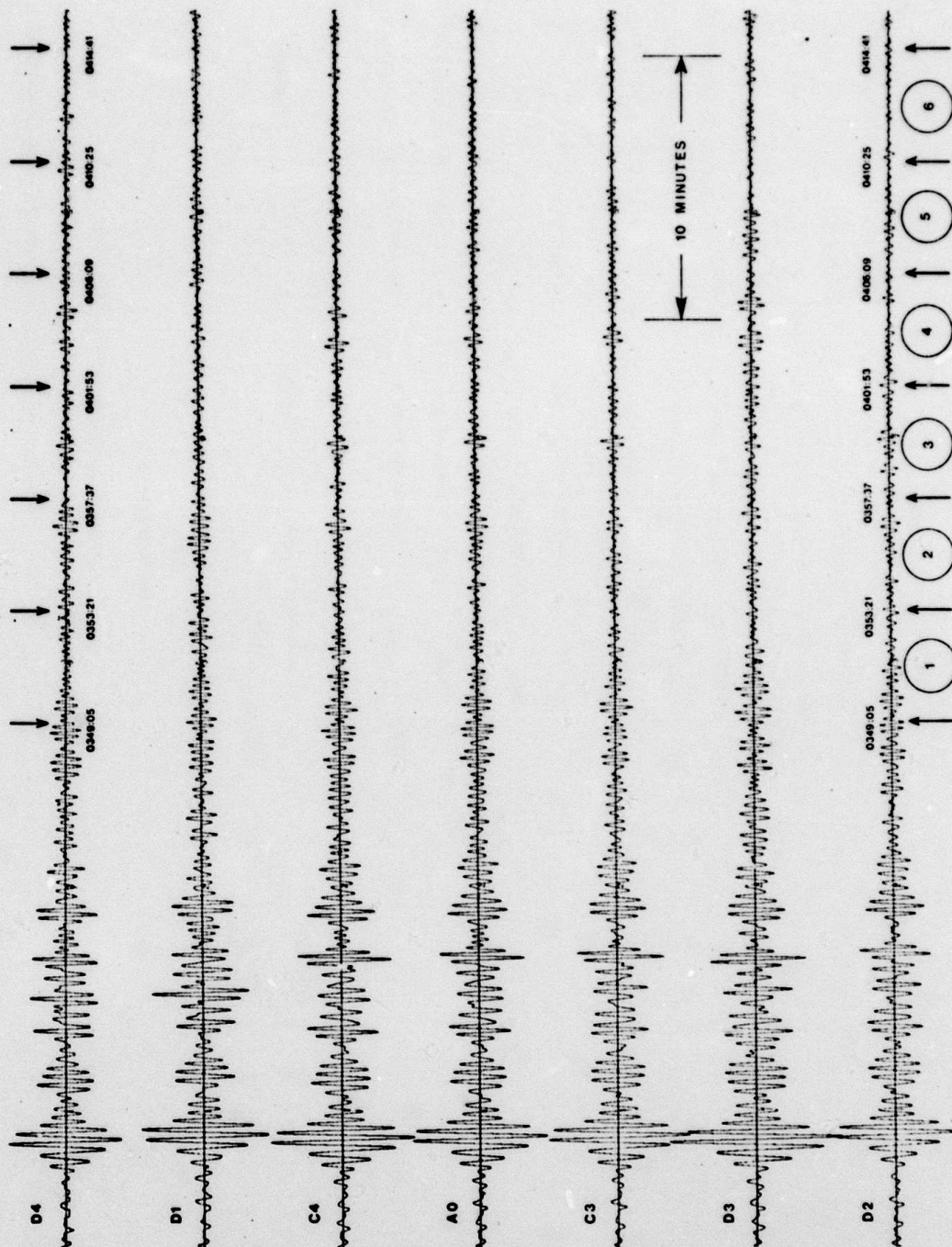


Figure 5. 0329:08 through 0415 GMT, 31MAY74. Seismograms from the LASA LP array (verticals). See page 36.

THE FOLLOWING BULLETIN PRESENTS THE RESULTS OF HIGH RESOLUTION FREQUENCY-WAVENUMBER ANALYSIS APPLIED TO THE DATA OF THE PRECEDING TIME SINGLES.

PERIOD IN SECONDS	APPARENT VELOCITY IN K/S	BACK AZIMUTH IN DEGREES EAST OF NORTH	PERIOD IN SECONDS	APPARENT VELOCITY IN K/S	BACK AZIMUTH IN DEGREES EAST OF NORTH	F-STATISTIC	F-STATISTIC
23.273	3.450	327	23.273	5.377	23	.324E 02	111
21.333	3.412	352	21.333	3.021	293	.195E 02	52
19.592	3.129	288	19.592	3.136	169	.215E 02	17
18.286	4.328	334	18.286	2.095	338	.155E 02	7
17.067	3.813	377	17.067	3.583	293	.532E 02	129
15.000	3.473	356	15.000	2.307	296	.215E 02	49

THERE ARE 6 VECTORS AT THE LEFT, ABOVE, HAVING F-STATISTICS GREATER THAN 10.0. A LEAST SQUARES FIT OF ALL 6 WAVENUMBER VECTORS TO A CONSTANT VELOCITY-AZIMUTH LINE THROUGH F-K SPACE YIELDED AN APPARENT PHASE VELOCITY OF 3.89 K/S AT 328 DEGREES, WITH AN RMS ERROR TO THE FIT OF .008 CYCLES/KM.

THE FOLLOWING LIST REPEATS, IN AZIMUTHAL ORDER, ALL THE ABOVE VECTORS AT THE LEFT HAVING F-STATISTICS GREATER THAN 10.0. FOR EACH VECTOR THE LAST COLUMN GIVES, IN DEGREES, THE DISTANCE FROM THE PRECEDING VECTOR.

AZIMUTH	SPEED	F-STAT	PERIOD	DEGREES
298	3.158	35	19.49	309.2
301	3.120	282	23.27	33.2
334	4.328	50	18.28	33.0
336	3.823	352	15.00	1.2
337	3.813	401	17.07	1.3
352	3.412	371	21.33	13.1

THE MOST ABUNDANT CONCENTRATION OF VECTORS IN THE ABOVE LIST IS 6 IS THAT OF THE GROUP OF 6 VECTORS BETWEEN 298 AND 352 DEGREES. THE EQUIVALENT OF 6 OR MORE OUT OF 6 VECTORS WITHIN 5.0 DEGREES OR LESS WILL OCCUR AT RANDOM ON THE AVERAGE 2.5% OF THE TIME. A LEAST SQUARES FIT OF ALL 6 WAVENUMBER VECTORS TO A CONSTANT VELOCITY-AZIMUTH LINE THROUGH F-K SPACE YIELDED AN APPARENT PHASE VELOCITY OF 3.69 K/S AT 328 DEGREES, WITH AN RMS ERROR TO THE FIT OF .008 CYCLES/KM.

THERE ARE 5 VECTORS AT THE RIGHT, ABOVE, HAVING F-STATISTICS GREATER THAN 10.0. A LEAST SQUARES FIT OF ALL 5 WAVENUMBER VECTORS TO A CONSTANT VELOCITY-AZIMUTH LINE THROUGH F-K SPACE YIELDED AN APPARENT PHASE VELOCITY OF 5.45 K/S AT 293 DEGREES, WITH AN RMS ERROR TO THE FIT OF .013 CYCLES/KM.

THE FOLLOWING LIST REPEATS, IN AZIMUTHAL ORDER, ALL THE ABOVE VECTORS AT THE RIGHT HAVING F-STATISTICS GREATER THAN 10.0. FOR EACH VECTOR THE LAST COLUMN GIVES, IN DEGREES, THE DISTANCE FROM THE PRECEDING VECTOR.

AZIMUTH	SPEED	F-STAT	PERIOD	DEGREES
293	5.377	111	23.27	87.0

Figure 6. 0349:05 to 0358:20 GMT, 31MAY74, LASA LP array.

THE FOLLOWING BULLETIN PRESENTS THE RESULTS OF HIGH RESOLUTION FREQUENCY-AVE NUMBER ANALYSIS APPLIED TO THE DATA OF THE PRECEDING TIME WINDOW.

PERIOD IN SECONDS	APPARENT VELOCITY IN K/S	BACK AZIMUTH IN DEGREES EAST OF NORTH	POWER	F-STATISTIC	PERIOD IN SECONDS	APPARENT VELOCITY IN K/S	BACK AZIMUTH IN DEGREES EAST OF NORTH	POWER	F-STATISTIC
23.273	4.077	323	.772	5	23.273	2.604	215	.954	7
21.333	2.530	341	.156	473	21.333	3.775	25	.192	17
19.292	3.152	325	.146	26	19.292	3.404	38	.182	28
17.257	3.833	305	.197	334	17.257	2.573	273	.392	55
15.220	3.334	303	.275	252	15.220	3.272	355	.695	119
					16.000	3.790	383	.579	23

THERE ARE 5 VECTORS AT THE LEFT, ABOVE, HAVING F-STATISTICS GREATER THAN 10.0. A LEAST SQUARES FIT OF ALL 5 AVE NUMBER VECTORS TO A CONSTANT VELOCITY-AZIMUTH LINE THROUGH F-K SPACE YIELDED AN APPARENT PHASE VELOCITY OF 3.442 K/S AT 319 DEGREES, WITH AN RMS ERROR TO THE FIT OF .005 CYCLES/KM.

THE FOLLOWING LIST REPEATS, IN AZIMUTHAL ORDER, ALL THE ABOVE VECTORS AT THE LEFT HAVING F-STATISTICS GREATER THAN 10.0. FOR EACH VECTOR THE LAST COLUMN GIVES, IN DEGREES, THE DISTANCE FROM THE PRECEDING VECTOR.

AZIMUTH	SPEED	F-STAT	PERIOD	DEGREES
303	3.334	252	15.00	322.1
305	3.152	325	17.07	1.4
323	4.077	473	21.33	18.7
325	3.152	26	19.29	1.4
341	2.530	25	16.69	15.4

THE MOST ANOMALOUS CONCENTRATION OF VECTORS IN THE ABOVE LIST OF 5 IS THAT OF THE GROUP OF 5 VECTORS BETWEEN 303 AND 341 DEGREES. THE EQUIVALENT OF 5 OR MORE OUT OF 5 VECTORS WITHIN 37.9 DEGREES OR LESS WILL OCCUR AT RANDOM ON THE AVERAGE 1 IN 16 DAYS. A LEAST SQUARES FIT OF ALL 5 AVE NUMBER VECTORS TO A CONSTANT VELOCITY-AZIMUTH LINE THROUGH F-K SPACE YIELDED AN APPARENT PHASE VELOCITY OF 3.442 K/S AT 319 DEGREES, WITH AN RMS ERROR TO THE FIT OF .005 CYCLES/KM.

THERE ARE 5 VECTORS AT THE RIGHT, ABOVE, HAVING F-STATISTICS GREATER THAN 10.0. A LEAST SQUARES FIT OF ALL 5 AVE NUMBER VECTORS TO A CONSTANT VELOCITY-AZIMUTH LINE THROUGH F-K SPACE YIELDED AN APPARENT PHASE VELOCITY OF 3.575 K/S AT 342 DEGREES, WITH AN RMS ERROR TO THE FIT OF .011 CYCLES/KM.

THE FOLLOWING LIST REPEATS, IN AZIMUTHAL ORDER, ALL THE ABOVE VECTORS AT THE RIGHT HAVING F-STATISTICS GREATER THAN 10.0. FOR EACH VECTOR THE LAST COLUMN GIVES, IN DEGREES, THE DISTANCE FROM THE PRECEDING VECTOR.

AZIMUTH	SPEED	F-STAT	PERIOD	DEGREES
25	3.775	17	21.33	37.2
38	3.404	38	19.69	13.5

Figure 7. 0353:21 to 0357:36 GMT, 31MAY74, LASA LP array.

THE FOLLOWING BULLETIN PRESENTS THE RESULTS OF HIGH RESOLUTION FREQUENCY-WAVELENGTH ANALYSIS APPLIED TO THE DATA OF THE PRECEDING TIME PERIOD.

PERIOD IN SECONDS	APPARENT VELOCITY IN K/S	BACK AZIMUTH IN DEGREES		POWER	F-STATISTIC	PERIOD IN SECONDS	APPARENT VELOCITY IN K/S	BACK AZIMUTH IN DEGREES		POWER	F-STATISTIC
		EAST OF NORTH	WEST OF NORTH					EAST OF NORTH	WEST OF NORTH		
23.273	3.715	344	818E 02	506	55	23.273	4.863	319	682E 01	203E 02	55
21.333	4.959	62	304E 03	753	52	21.333	6.555	75	203E 02	203E 02	52
19.692	2.210	324	705E 02	70	17	19.692	4.025	345	322E 02	322E 02	17
18.286	3.650	298	572E 02	202	48	18.286	2.453	356	531E 02	531E 02	48
17.097	4.339	319	734E 02	118	57	17.097	3.038	343	227E 02	227E 02	57
16.000	3.413	313	695E 02	176		16.000	3.038	343	227E 02	227E 02	

THERE ARE 6 VECTORS AT THE LEFT, ABOVE, HAVING F-STATISTICS GREATER THAN 10.0. A LEAST SQUARES FIT OF ALL 6 WAVELENGTH VECTORS TO A CONSTANT VELOCITY-AZIMUTH LINE THROUGH F-K SPACE YIELDED AN APPARENT PHASE VELOCITY OF 4.089 K/S AT 323 DEGREES, WITH AN RMS ERROR TO THE FIT OF .009 CYCLES/KM.

THE FOLLOWING LIST REPEATS, IN AZIMUTHAL ORDER, ALL THE ABOVE VECTORS AT THE LEFT HAVING F-STATISTICS GREATER THAN 10.0. FOR EACH VECTOR THE LAST COLUMN GIVES, IN DEGREES, THE DISTANCE FROM THE PRECEDING VECTOR.

AZIMUTH	SPEED	F-STAT	PERIOD	DEGREES
62	4.989	753	21.33	78.0
298	3.650	202	18.29	236.0
313	3.413	176	16.00	1.0
318	4.635	118	17.07	3.0
324	2.210	70	19.69	5.5
344	3.715	505	23.27	20.2

THERE ARE 6 VECTORS AT THE RIGHT, ABOVE, HAVING F-STATISTICS GREATER THAN 10.0. A LEAST SQUARES FIT OF ALL 6 WAVELENGTH VECTORS TO A CONSTANT VELOCITY-AZIMUTH LINE THROUGH F-K SPACE YIELDED AN APPARENT PHASE VELOCITY OF 2.923 K/S AT 341 DEGREES, WITH AN RMS ERROR TO THE FIT OF .014 CYCLES/KM.

THE FOLLOWING LIST REPEATS, IN AZIMUTHAL ORDER, ALL THE ABOVE VECTORS AT THE RIGHT HAVING F-STATISTICS GREATER THAN 10.0. FOR EACH VECTOR THE LAST COLUMN GIVES, IN DEGREES, THE DISTANCE FROM THE PRECEDING VECTOR.

AZIMUTH	SPEED	F-STAT	PERIOD	DEGREES
75	6.556	502	21.33	79.1
319	4.863	55	23.27	243.9
324	1.100	57	19.69	4.5
343	3.038	57	16.00	19.5
345	4.025	117	18.29	2.4
356	2.453	48	17.07	10.9

Figure 8. 0357:37 to 0401:52 GMT, 31MAY74, LASA LP array.

THE FOLLOWING BULLETIN PRESENTS THE RESULTS OF HIGH RESOLUTION FREQUENCY-AVE NUMBER ANALYSIS APPLIED TO THE DATA OF THE PRECEDING TIME BINS.

PERIOD SECONDS	APPARENT VELOCITY IN K/S	BACK AZIMUTH IN DEGREES EAST OF NORTH	POWER	F-STATISTIC	PERIOD IN SECONDS	APPARENT VELOCITY IN K/S	BACK AZIMUTH IN DEGREES EAST OF NORTH	POWER	F-STATISTIC
23.273	3.554	297	.502E 01	30	23.273	1.531	201	.282E 01	17
21.333	3.546	31	.128E 03	372	21.333	3.585	280	.312E 02	32
19.892	3.747	315	.118E 03	98	19.892	4.173	21	.372E 02	74
18.265	4.345	33	.550E 02	125	18.265	1.755	15	.556E 01	12
17.587	4.027	32	.166E 02	60	17.587	3.452	334	.142E 02	53
16.000	3.289	329	.547E 02	85	16.000	3.289	329	.255E 02	54

THERE ARE 6 VECTORS AT THE LEFT, ABOVE HAVING F-STATISTICS GREATER THAN 10.0. A LEAST SQUARES FIT OF ALL 6 AVE NUMBER VECTORS TO A CONSTANT VELOCITY-AZIMUTH LINE THROUGH F-K SPACE YIELDED AN APPARENT PHASE VELOCITY OF .0715 K/S AT 353 DEGREES, WITH AN RMS ERROR TO THE FIT OF .009 CYCLES/KM.

THE FOLLOWING LIST REPEATS, IN AZIMUTHAL ORDER, ALL THE ABOVE VECTORS AT THE LEFT HAVING F-STATISTICS GREATER THAN 10.0. FOR EACH VECTOR THE LAST COLUMN GIVES, IN DEGREES, THE DISTANCE FROM THE PRECEDING VECTOR.

AZIMUTH	SPEED	F-STAT	PERIOD	DEGREES
31	3.646	372	21.33	61.8
32	4.027	60	17.07	.7
33	4.345	125	18.29	1.0
297	3.554	30	23.27	264.2
316	3.747	98	19.89	19.1
329	3.289	85	16.00	13.2

THERE ARE 6 VECTORS AT THE RIGHT, ABOVE, HAVING F-STATISTICS GREATER THAN 10.0. A LEAST SQUARES FIT OF ALL 6 AVE NUMBER VECTORS TO A CONSTANT VELOCITY-AZIMUTH LINE THROUGH F-K SPACE YIELDED AN APPARENT PHASE VELOCITY OF .07892 K/S AT 335 DEGREES, WITH AN RMS ERROR TO THE FIT OF .018 CYCLES/KM.

THE FOLLOWING LIST REPEATS, IN AZIMUTHAL ORDER, ALL THE ABOVE VECTORS AT THE RIGHT HAVING F-STATISTICS GREATER THAN 10.0. FOR EACH VECTOR THE LAST COLUMN GIVES, IN DEGREES, THE DISTANCE FROM THE PRECEDING VECTOR.

AZIMUTH	SPEED	F-STAT	PERIOD	DEGREES
16	3.756	12	18.29	40.8

Figure 9. 0401:53 to 0406:08 GMT, 31MAY74, LASA LP array.

THE FOLLOWING BULLETIN PRESENTS THE RESULTS OF HIGH RESOLUTION FREQUENCY-AVE NUMBER ANALYSIS APPLIED TO THE DATA OF THE PRECEDING TIME INTERVAL.

PERIOD IN SECONDS	APPARENT VELOCITY IN K/S	BACK AZIMUTH IN DEGREES EAST OF NORTH	F-STATISTIC	ORDER	PERIOD IN SECONDS	APPARENT VELOCITY IN K/S	BACK AZIMUTH IN DEGREES EAST OF NORTH	F-STATISTIC	ORDER
23.273	3.013	118	19	02	23.273	2.125	215	6	01
21.333	4.845	20	2575	03	21.333	4.267	358	276	02
19.692	2.642	313	151	02	19.692	2.700	79	41	02
18.286	1.717	40	49	02	18.286	1.137	46	17	01
17.067	3.977	97	38	02	17.067	2.336	62	16	02
16.000	2.330	274	47	02	16.000	3.203	341	46	02

THERE ARE 5 VECTORS AT THE LEFT, ABOVE, HAVING F-STATISTICS GREATER THAN 10.0. A LEAST SQUARES FIT OF ALL 6 AVE NUMBER VECTORS TO A CONSTANT VELOCITY-AZIMUTH LINE THROUGH F-K SPACE YIELDED AN APPARENT PHASE VELOCITY OF 3.643 K/S AT 356 DEGREES, WITH AN RMS ERROR TO THE FIT OF .017 CYCLES/KM.

THE FOLLOWING LIST REPEATS IN AZIMUTHAL ORDER, ALL THE ABOVE VECTORS AT THE LEFT HAVING F-STATISTICS GREATER THAN 10.0. FOR EACH VECTOR THE LAST COLUMN GIVES IN DEGREES, THE DISTANCE FROM THE PRECEDING VECTOR.

AZIMUTH	SPEED	F-STAT	PERIOD	DEGREES
3	3.977	38	17.07	49.7
20	4.845	2575	21.33	17.0
40	1.783	49	18.29	20.9
118	3.118	19	23.27	77.3
274	2.330	47	16.00	155.3
313	2.642	151	19.69	35.3

THERE ARE 5 VECTORS AT THE RIGHT, ABOVE, HAVING F-STATISTICS GREATER THAN 10.0. A LEAST SQUARES FIT OF ALL 6 AVE NUMBER VECTORS TO A CONSTANT VELOCITY-AZIMUTH LINE THROUGH F-K SPACE YIELDED AN APPARENT PHASE VELOCITY OF 2.601 K/S AT 40 DEGREES, WITH AN RMS ERROR TO THE FIT OF .018 CYCLES/KM.

THE FOLLOWING LIST REPEATS IN AZIMUTHAL ORDER, ALL THE ABOVE VECTORS AT THE RIGHT HAVING F-STATISTICS GREATER THAN 10.0. FOR EACH VECTOR THE LAST COLUMN GIVES IN DEGREES, THE DISTANCE FROM THE PRECEDING VECTOR.

AZIMUTH	SPEED	F-STAT	PERIOD	DEGREES
46	1.137	17	18.29	98.0
62	2.636	16	17.07	15.0
79	2.700	41	19.69	17.5
341	3.203	46	16.00	261.5
358	4.267	276	21.33	17.0

Figure 10. 0406:09 to 0410:24 GMT, 31MAY74, LASA LP array.

THE FOLLOWING BULLETIN PRESENTS THE RESULTS OF HIGH RESOLUTION FREQUENCY-AVENUMBER ANALYSIS APPLIED TO THE DATA OF THE PRECEDING TIME INTERVAL.

PERIOD IN SECONDS	APPARENT PHASE VELOCITY IN K/M/S	BACK AZIMUTH IN DEGREES EAST OF NORTH	POWER	F-STATISTIC	PERIOD IN SECONDS	APPARENT PHASE VELOCITY IN K/M/S	BACK AZIMUTH IN DEGREES EAST OF NORTH	POWER	F-STATISTIC
23.273	4.337	79	.163E 02	91	23.273	5.154	183	.162E 02	59
21.333	3.830	351	.098E 02	148	21.333	2.913	185	.422E 01	22
19.692	4.259	282	.093E 02	229	19.692	3.668	359	.131E 02	67
18.285	3.680	351	.075E 02	217	18.285	3.535	322	.433E 02	107
17.167	3.077	312	.013E 02	37	17.067	2.513	91	.855E 01	15
16.000	3.351	254	.025E 01	25	16.000	2.542	175	.332E 01	22

THERE ARE 6 VECTORS AT THE LEFT, ABOVE, HAVING F-STATISTICS GREATER THAN 10.0. A LEAST SQUARES FIT OF ALL 6 AVEUMBER VECTORS TO A CONSTANT VELOCITY-AZIMUTH LINE THROUGH F-K SPACE YIELDED AN APPARENT PHASE VELOCITY OF 3.201 K/M/S AT 313 DEGREES, WITH AN RMS ERROR TO THE FIT OF .011 CYCLES/KM.

THE FOLLOWING LIST REPEATS, IN AZIMUTHAL ORDER, ALL THE ABOVE VECTORS AT THE LEFT HAVING F-STATISTICS GREATER THAN 10.0. FOR EACH VECTOR THE LAST COLUMN GIVES, IN DEGREES, THE DISTANCE FROM THE PRECEDING VECTOR.

AZIMUTH	SPEED	F-STAT	PERIOD	DEGREES
75	4.333	91	23.27	83.9
254	3.830	29	16.00	179.3
312	3.077	37	17.07	57.3
322	4.036	229	19.69	3.5
351	3.680	217	18.28	23.3
351	3.350	143	21.33	4.5

THERE ARE 6 VECTORS AT THE RIGHT, ABOVE, HAVING F-STATISTICS GREATER THAN 10.0. A LEAST SQUARES FIT OF ALL 6 AVEUMBER VECTORS TO A CONSTANT VELOCITY-AZIMUTH LINE THROUGH F-K SPACE YIELDED AN APPARENT PHASE VELOCITY OF 2.737 K/M/S AT 118 DEGREES, WITH AN RMS ERROR TO THE FIT OF .018 CYCLES/KM.

THE FOLLOWING LIST REPEATS, IN AZIMUTHAL ORDER, ALL THE ABOVE VECTORS AT THE RIGHT HAVING F-STATISTICS GREATER THAN 10.0. FOR EACH VECTOR THE LAST COLUMN GIVES, IN DEGREES, THE DISTANCE FROM THE PRECEDING VECTOR.

AZIMUTH	SPEED	F-STAT	PERIOD	DEGREES
31	2.648	15	17.07	32.5
175	2.512	22	16.00	14.2
185	5.154	80	23.27	7.9
195	2.913	22	21.33	2.1
322	3.668	107	18.28	130.9
359	3.535	67	19.69	36.5

Figure 11. 0410:25 to 0414:40 GMT, 31MAY74, LASA LP array.

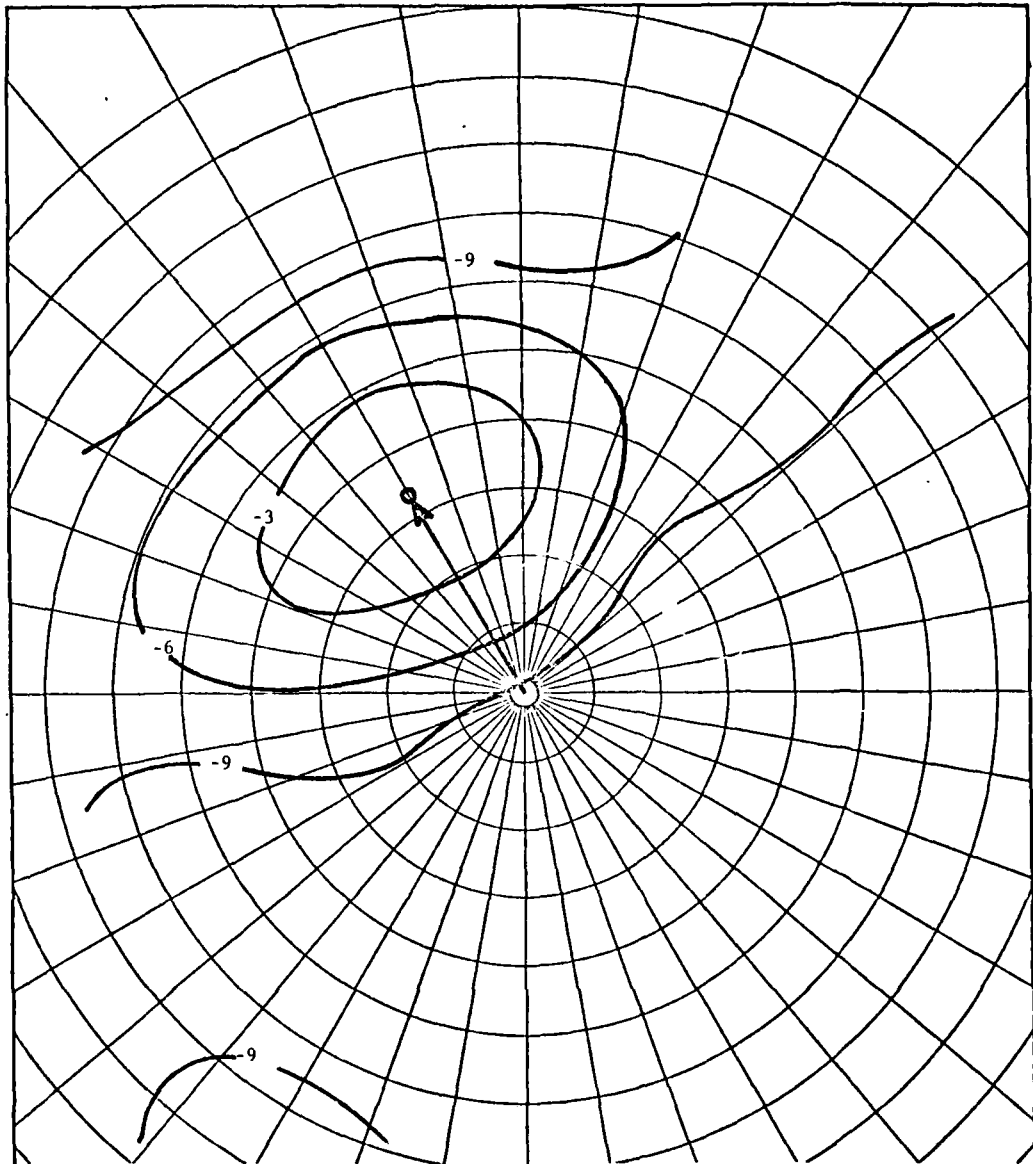
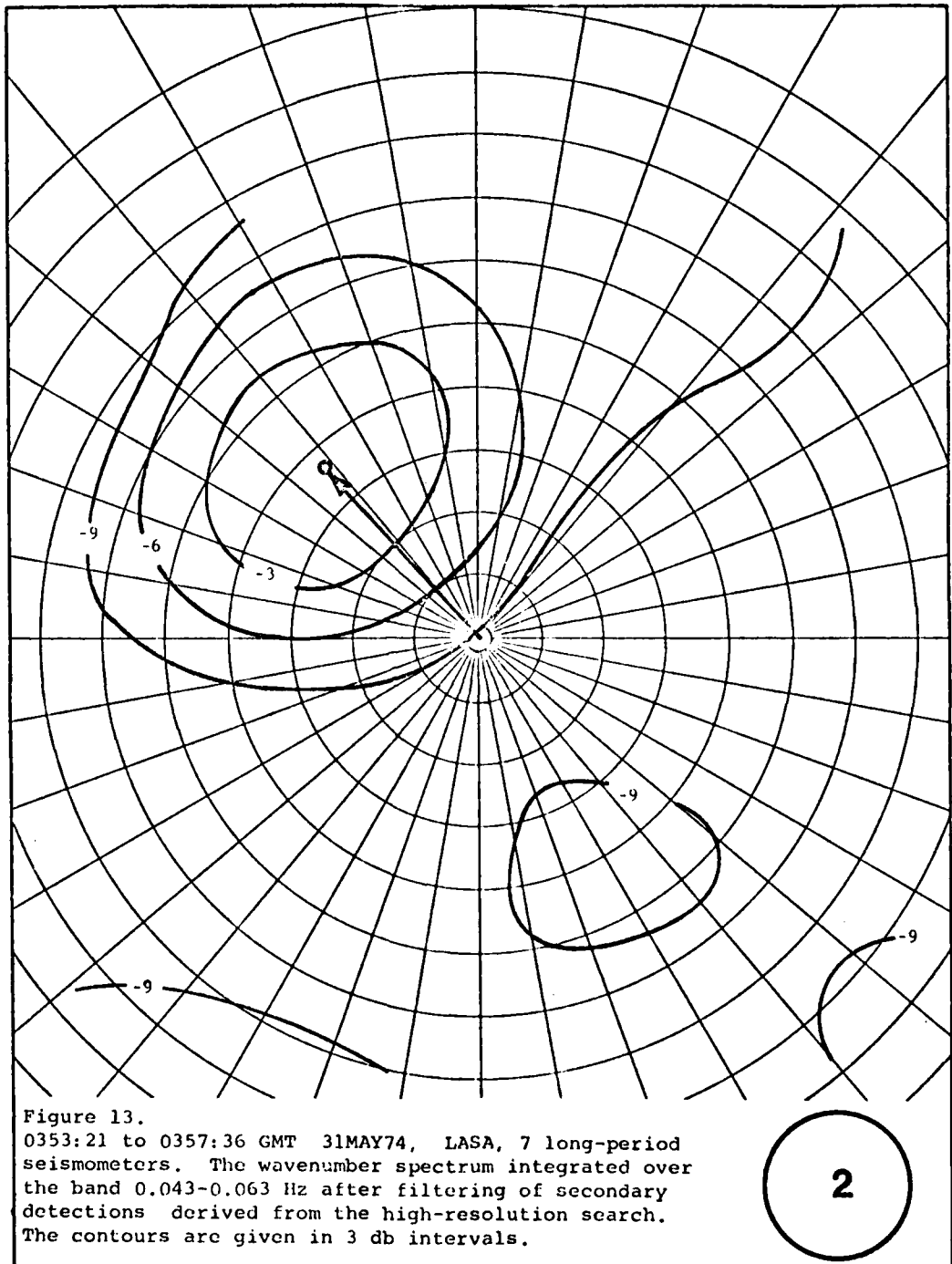


Figure 12.
0349:05 to 0353:20 GMT 31MAY74, LASA, 7 long-period
seismometers. The wavenumber spectrum integrated over
the band 0.043-0.063 Hz after filtering of secondary
detections derived from the high-resolution search.
The contours are given in 3 db intervals. The compon-
ent spectra have been normalized.

1



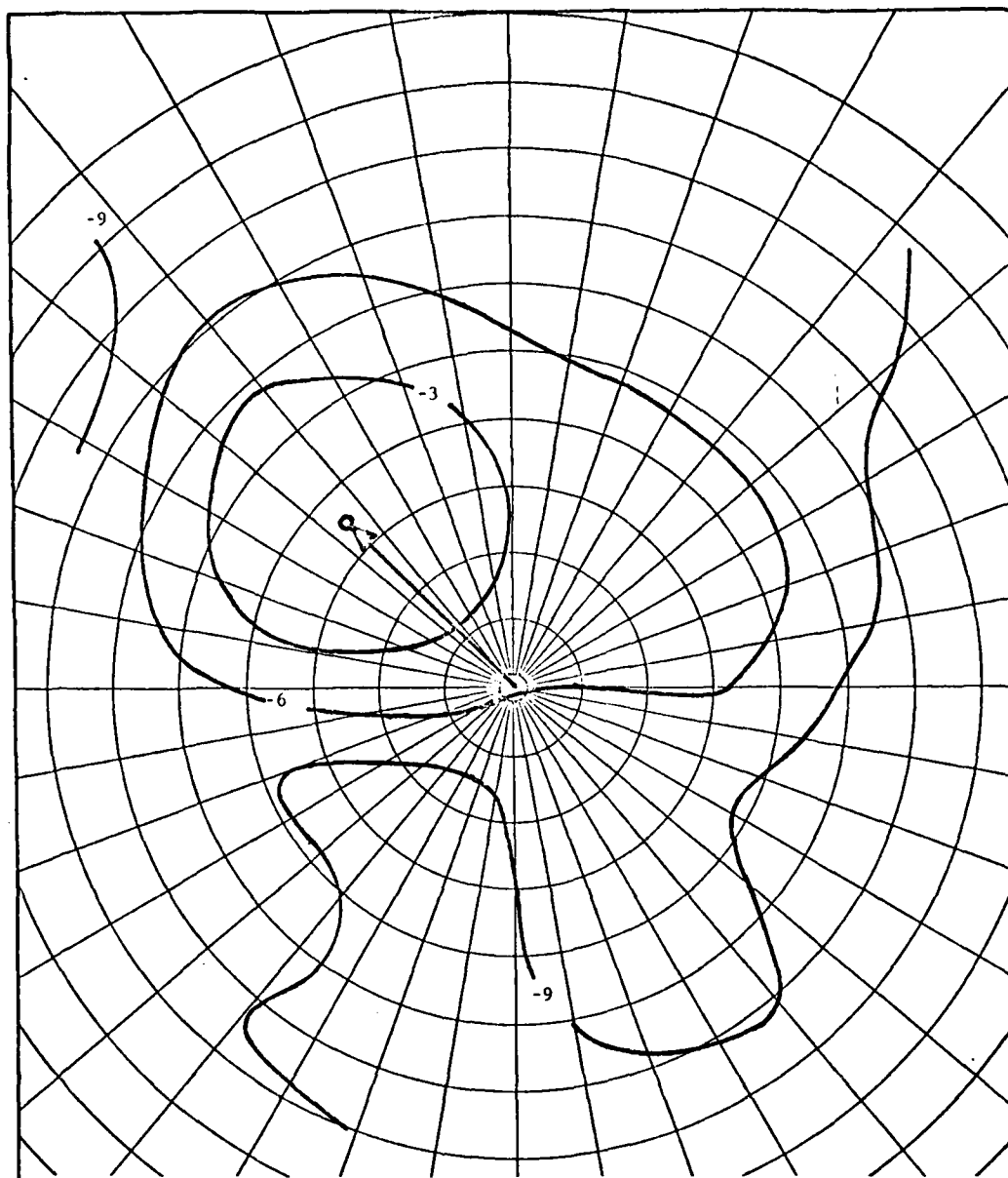


Figure 14.
0357:37 to 0401:52 GMT 31MAY74, LASA, 7 long-period
seismometers. The wavenumber spectrum integrated over
the band 0.043-0.063 Hz after filtering of secondary
detections derived from the high-resolution search.
The contours are given in 3 db intervals.

3

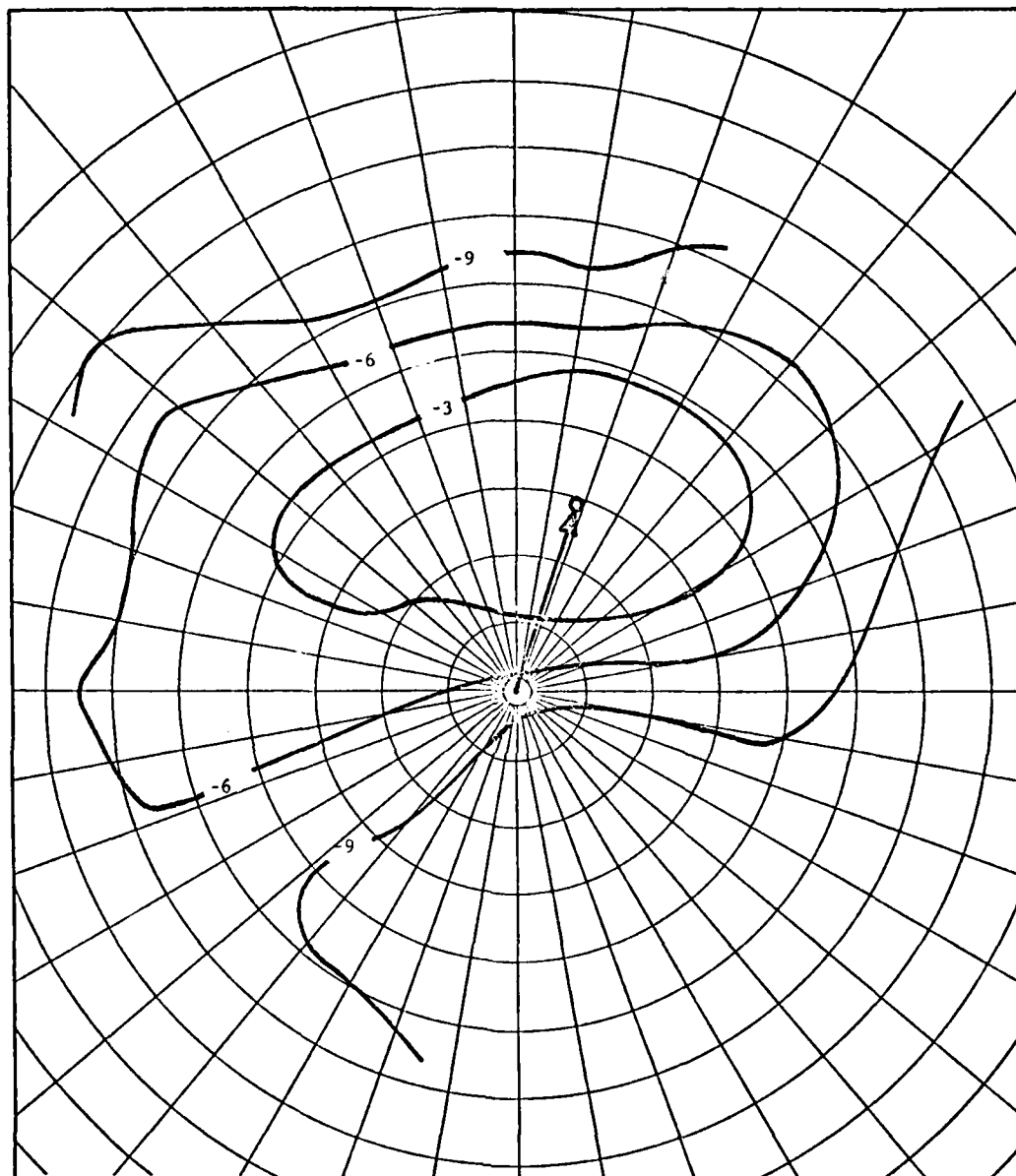
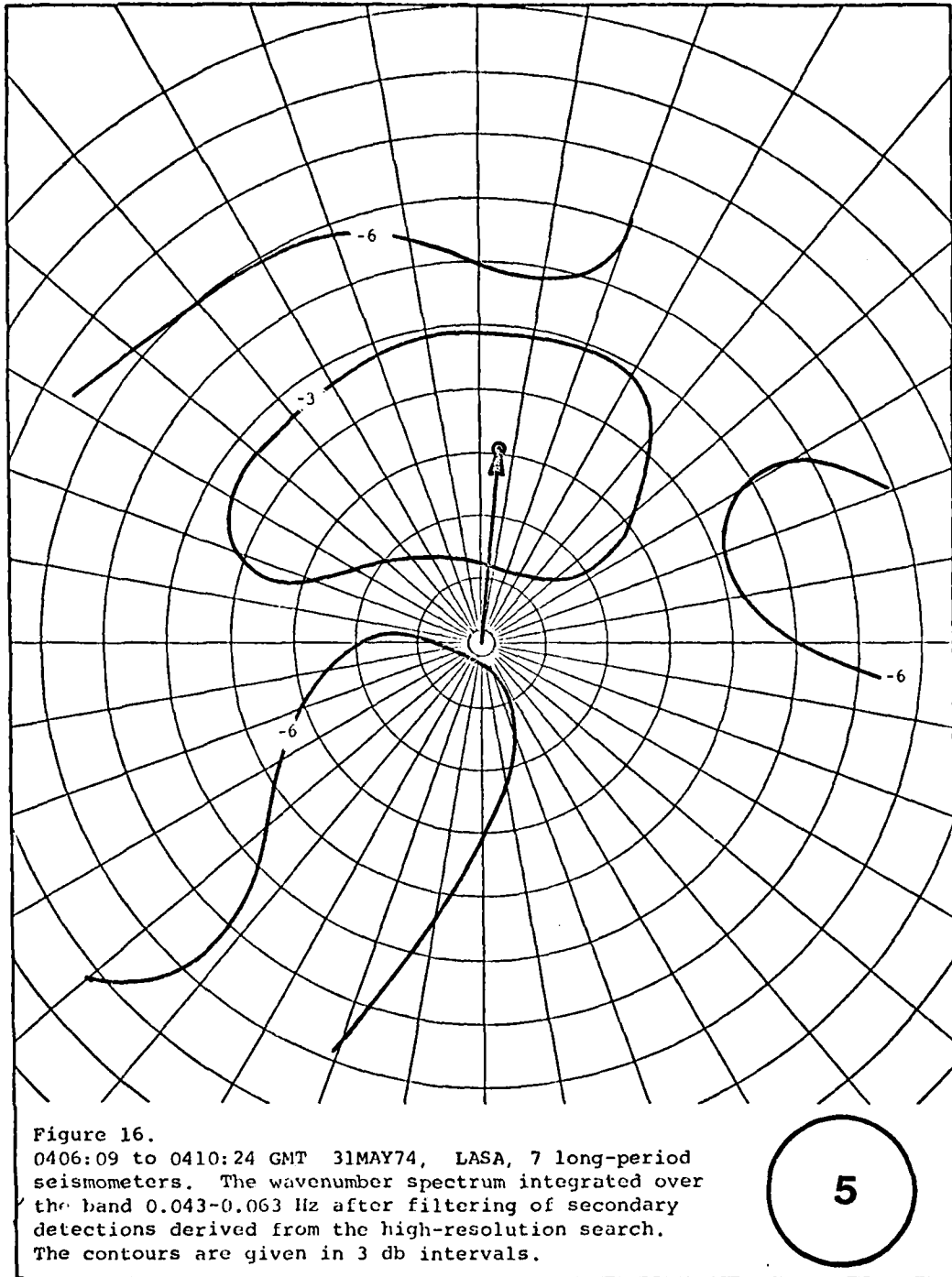


Figure 15.
0401:53 to 0406:08 GMT 31MAY74, LASA, 7 long-period
seismometers. The wavenumber spectrum integrated over
the band 0.043-0.063 Hz after filtering of secondary
detections derived from the high-resolution search.
The contours are given in 3 db intervals.

4



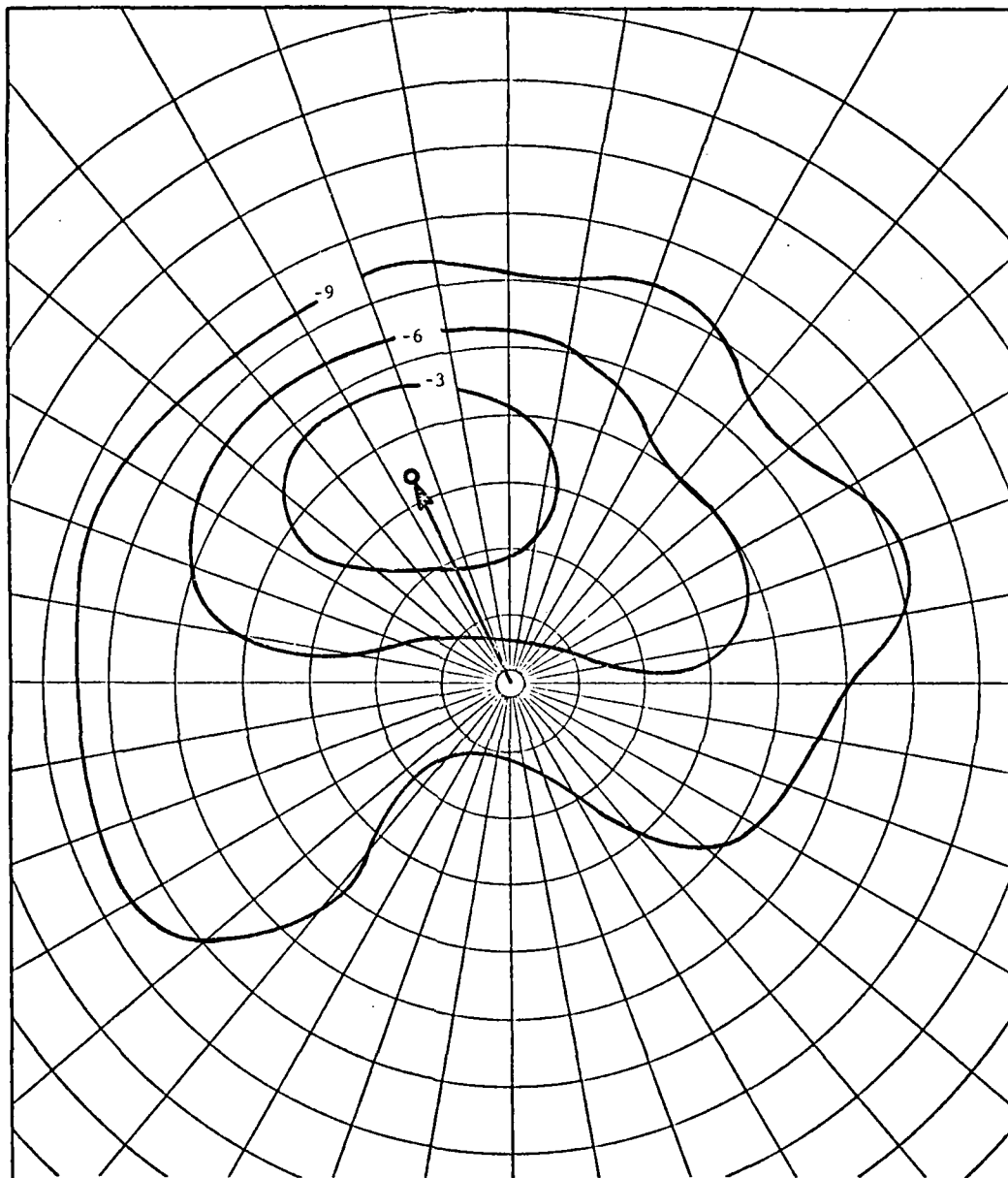


Figure 17.
0410:25 to 0414:40 GMT 31MAY74, LASA, 7 long-period
seismometers. The wavenumber spectrum integrated over
the band 0.043-0.063 Hz after filtering of secondary
detections derived from the high-resolution search.
The contour intervals are in 3 db steps.

6

BIBLIOGRAPHY

- 1.*Barnard, T.E., 1969, Analytical studies of techniques for the computation of high-resolution wavenumber spectra: Advanced Array Research Special Report No. 9, Dallas, Texas, Texas Instruments, Inc.
- 2.*Binder, F.H., 1968, Large-array signal and noise analysis: Quarterly Report No. 6, Dallas, Texas, Texas Instruments, Inc.
- 3.*Binder, F.H. and Peebles, J.R., 1968, Epicentral estimation for five LASA events using frequency-wavenumber spectra: Special Scientific Report No. 21, Dallas, Texas, Texas Instruments, Inc.
4. Barn, M. and Wolf, E., 1959, Principles of optics: Pergamon, London.
5. Burg, J.P., 1964, Three dimensional filtering with an array of seismometers: Geophysics, V. 29, No. 5, p. 693-713, October.
- 6.*Burg, J.P. and Burrell, G.C., 1967, Analysis of K-line wavenumber spectra from the TFO long noise sample: Array Research Special Report No. 23, Dallas, Texas, Texas Instruments, Inc.
- 7.*Burg, J.P., 1968, An evaluation of the use of high resolution wavenumber spectra for ambient noise analysis: Special Report No. 8, Dallas, Texas, Texas Instruments, Inc.
- 8.*Capon, J., 1968, Investigation of long period noise at LASA: Technical Note 1968-15, Lexington, Mass., Lincoln Laboratory MIT.
9. Capon, J. 1969, High resolution frequency-wavenumber spectrum analysis: Proc. IEEE, V. 57, No. 8, p. 140-1418, August.
10. Capon, J. and Goodman, N.R., 1970, Probability distribution for estimators of the frequency-wavenumber spectrum: Proc. IEEE letters, V. 58, No. 10. p. 1785-1786, October.
11. Cox, H., 1973, Resolving power and sensitivity to mismatch of optimum array processors: J. Acoust. Soc. Am., V. 54, No. 3, p. 771-785, September.
- 12.*Crouch, D.B. and Binder, F.H., 1967, Analysis of subarray wavenumber spectra: Special Scientific Report No. 6,

Dallas, Texas, Texas Instruments, Inc.

- 13.*Galat, G. and Sax, R., 1969, Horizontal array response of several wavenumber analysis methods: Seismic Data Laboratory Report No. 244, Alexandria, Virginia, Teledyne Geotech.
- 14.*Haney, W.P., 1967, Research on high -resolution frequency wavenumber spectra: Special Scientific Report No. 2, Dallas, Texas, Texas Instruments, Inc.
- 15.*Lintz, P.R., 1968, An analysis of a technique for the generation of high-resolution wavenumber spectra: Seismic Data Laboratory Report No. 218, Alexandria, Virginia, Teledyne Geotech.
16. Martin, J. Jr., 1972, Address to the plenary session in Geneva, August 24: CCD/PV. 580, United Nations, New York.
- 17.*McCowan, D.W. and Lintz, P.R., 1968, High-resolution frequency wavenumber spectra: Seismic Data Laboratory Report No. 206, Alexandria, Virginia, Teledyne Geotech.
18. McDonough, R.N., 1972, Degraded performance of nonlinear array processors in the presence of data modeling errors: J. Acoust. Soc. Am., V. 51, No. 4, p. 1186-1193, April.
- 19.*Ong, C., and Laster, S., 1971, High resolution wavenumber spectra, special scientific Report No. 1, Dallas, Texas, Texas Instruments, Incorporated.
20. Seligson, C.D., 1970, Comments on high resolution frequency-wave number spectrum analysis: Proc. IEEE, V. 58, No. 6, p. 947-949, June.
21. Wilkins, W.S., Heiting, L.N. and Binder, F.H., 1968, Location statistics for frequency-wavenumber processings: Special Scientific Report No. 25, Dallas, Texas, Texas Instruments, Incorporated.
22. Woods, J.W., 1972, Two-dimensional discrete markovian random fields: IEEE Trans. on Inf. Th., V. IT-18, No. 2, March.
23. Woods, J.W. and Lintz, P.R., 1972, Plane waves at small arrays: Technical Note No. 32, Alexandria Virginia, VSC Air Force Technical Applications Center.

24. Mack, H., and Smart, E., 1972, Automatic processing of multi-array long-period seismic data, Geophys. J. of Roy Astro. Soc., V. 35, nos. 1-3, December, 1973.

* Available from Clearinghouse for Federal Scientific and Technical Information, U.S. Dept. of Commerce, Springfield, Virginia 22151.